NRL Report 6649

The Tensile Properties of Selected Steels for Use in Nuclear Reactor Pressure Vessels

EUGENE P. KLIER, J. R. HAWTHORNE, AND LENDELL E. STEELE

Reactor Materials Branch
Metallurgy Division

December 26, 1967

NAVAL RESEARCH LABORATORY
Washington, D.C.

This document has been approved for public release and sale; its distribution is unlimited.

CONTENTS

Abstract	ii
Problem Status	ii
Authorization	ii
INTRODUCTION	1
EXPERIMENTAL PROCEDURE	2
Materials	2
Tensile Specimens and Testing Procedures	2
Metallography	5
Representation of the Test Data	5
METALLOGRAPHIC STRUCTURES	5
TENSILE PROPERTIES	8
Specimen Orientation	8
Processing History	9
Steel Composition	11
Neutron Fluence Exposure	13
Tensile Specimen Fractures	22
DISCUSSION OF RESULTS	24
SUMMARY	26
ACKNOWLEDGMENTS	27
REFERENCES	27
APPENDIX – Summary Tables and Plots of Data Envelopes	30

ABSTRACT

Seven steels now used or having potential for use in the construction of nuclear reactor containment vessels were evaluated in uniaxial tension at 75°F following irradiation at < 250°F. Experiment irradiations involved neutron fluences up to 9.5×10^{19} n/cm^2 (> 1 Mev). Tensile properties of the A212-B, A302-B, A350-LF1 (Modified), A350-LF3, A353, T-1, and HY-80 (Ni-Cr-Mo) steels were determined as conventional tensile and yield strength and percent reduction of area. In addition, observed stress-strain relationships were plotted using both nominal stress-percent reduction of area coordinates and true stress-natural strain coordinates. Curves given in the latter coordinate system were also expressed in suitable analytic form. All individual tensile data were compiled in tabular form, and stress-strain curves were summarized as bands giving maximum and minimum properties behavior.

Limited metallographic and fractographic data were obtained to establish the metallurgical structures of the steels and to depict the transition from a ductile shear fracture to a brittle flat fracture at high neutron fluences for the more brittle steels.

PROBLEM STATUS

This report covers one phase of the work; work on other phases is continuing.

AUTHORIZATION

NRL Problem M01-14
Projects RR 007-01-46-5409 and SF 020-01-05-0858
AEC-AT(49-5)-2110; USA-ERG-3-67

Manuscript submitted September 22, 1967.

THE TENSILE PROPERTIES OF SELECTED STEELS FOR USE IN NUCLEAR REACTOR PRESSURE VESSELS

INTRODUCTION

Power reactor pressure vessels because of boiler code restrictions have until recently been projected as being constructed of A302-B steel (1), a modified Mn-Mo steel which in the heavy-thickness plates (to 12 inches) required, transforms on quenching to mixtures of martensite and bainite. For plate thicknesses above 12 inches, however, this steel is not suitable for projected pressure vessel applications because of the inferior fracture toughness observed for the heavier sections. To facilitate construction of the projected larger nuclear power plants, new higher strength steels are needed such as the recently approved ASTM A543 steel, which is more generally known as HY-80, a steel developed for submarine construction. Through use of this steel a hypothetical 3000-Mwe pressure vessel, which would require a wall thickness of 12 inches if fabricated of A302-B steel, could have a wall thickness of 10 inches, leading to a weight saving of 500 to 750 tons for the pressure vessel (1). For higher strength steels additional savings in weight become possible along with a superior fracture toughness. This superior toughness is retained with less modification indicated on exposure to neutron flux environments (2) than is the case for A302-B steel. It has been suggested by Steele et al. (2) that, for the plate thicknesses of concern in pressure vessel applications with an increase in tensile strength, there is in general observed a lower initial NDT, a smaller ΔNDT with neutron exposure, and a possible earlier saturation of the radiation damage effect.

Possible application of the higher strength materials to nuclear pressure vessel construction would appear to be limited in the near future to HY-80 steel. This steel is competitive economically, and it has been extensively applied in constructing high performance naval vessels. Consequently, the fabrication characteristics and requirements of the steel are well established.* However, to develop suitable background information for evaluating the response of high strength steel to neutron exposure, it is desirable to establish the tensile properties changes of such steels with various chemical compositions and initial tensile strengths with progressively increasing neutron exposures. At the present time the tensile data taken for steels other than A212-B and A302-B, both of which are minimum strength steels for pressure vessel applications, have been confined largely to conventional tensile data. These data have been reviewed at some length by Trudeau (3). In general the yield strength of a steel is elevated on continued exposure to a fission neutron environment, and the rate of increase of the yield strength is represented frequently by a relation of the form (4)†

$$\Delta\sigma_{ys} = A\sqrt{\phi t} ,$$

where $\Delta\sigma_{ys}$ is the increase in σ_{ys} in ksi, A is a constant, and ϕt is the neutron flux in units of 10^{18}. The proportionating constant A in this expression will vary in magnitude

*This statement while valid for nonradiated steels, may require reconsideration for nuclear applications. Preliminary data have indicated a high sensitivity to radiation of conventional HY-80 weldments.

†This relationship is frequently challenged and can be only approximately correct on extrapolation to high neutron fluences.

with structure of the steel and the temperature of testing; for steels such as those tested in the present study A has been reported (5) to vary from about 16 for an exposure temperature of 100°C to about 2 for an exposure temperature of 350°C. However, a suitable functional relationship between A and exposure and test temperature has not as yet been developed.

The true stress-natural strain properties of steels following radiation damage have been employed by Trozera and Flynn (6) in the study of failure conditions in tubes after radiation damage. Examination of their results suggests that, in general, the analysis of structural failure due to the action of multiaxial stresses requires the use of suitable generalized stress-strain relations such as the true stress-natural strain relations. Such relations where expressed in the analytic form $\sigma = \sigma_0 \delta^n$ have been advanced by Cottrell (7) as suitable for the determination of σ_i and ky in the Petch (8) expression

$$\sigma_y = \sigma_i + ky/\sqrt{d} ,$$

where σ_y is the lower yield strength, ky is the dislocation locking stress, d is the grain diameter, and σ_i is the stress at the intersection of the elastic and plastic stress-strain curves. The values of σ_y, ky, and σ_i each is potentially a measure of radiation hardening. While σ_y is directly observable, the determination of ky requires the use of the true stress-natural strain properties of the steels.

Because of the possible theoretical as well as practical uses of the data, the tensile studies for the seven steels investigated have been completed to allow the true stress-natural strain data to be represented both graphically and analytically.

EXPERIMENTAL PROCEDURE

Materials

The low alloy constructional steels as a group are heat-treatable to microstructural conditions generally designated as ferritic (combined with pearlite), bainitic, and/or martensitic. These structures, which are formed on quenching, are more or less modified by tempering, but, for the most part, establish a maximum hardness and consequent tensile strength obtainable in the steel. Low strength levels are usually associated with the ferrite-pearlite microstructures, while intermediate and higher strength levels are associated with bainites and martensites.

For the present series, three steels form pearlite in ferrite; one transforms to a nearly homogeneous bainite structure throughout a plate thickness of 6 inches, while the remaining three steels transform to martensite. In addition, two series of steels with a complete range in microstructures can be established within this series by reference to nickel content as: less than about 0.5% and greater than about 1.75%. The compositions of the seven steels forming the series are given in Table 1. These steels at the indicated plate thicknesses were heat treated and then sectioned for specimen preparation.

Tensile Specimens and Testing Procedures

Tensile specimens of the dimensions given in Fig. 1 were prepared for encapsulation and exposure in selected neutron environments by the procedures that have been described at length in earlier reports (9-11). The specimen shape which has proven most convenient for determination of the load-diameter curve is designated in Fig. 1, and this is at present considered the standard shape. Specimens with a straight cylindrical test section complicate the procedures required to record the load-diameter curve in the test; these specimens are no longer made.

Table 1
Compositions and Heat Treated Conditions of the Steels

	Type of Steel	Chemical Analysis (wt-%)										Heat Treatments
		C	Mn	Si	P	S	Ni	Cr	Mo	V	Al	
Low Nickel Steels	A212-B (4-in.)	0.25	0.76	0.21	0.011	0.036	0.23	0.11	0.05	–	–	1650°F for 2 hr; water quenched; tempered 1175°F for 4 hr; furnace cooled to 600°F. (a) 1200°F temper.
		0.25	0.76	0.21	0.011	0.036	0.23	0.11	0.05	–	–	
		0.26	0.76	0.24	0.011	0.031	0.22	0.20	0.02	–	–	
		(a) 0.29	0.80	0.26	0.015	0.023	–	–	–	–	–	
	A302-B (6-in.)	0.23	1.35	0.22	0.015	0.021	0.22	0.12	0.52	–	–	1650°F for 2 hr; water quenched; tempered 1200°F for 6 hr; furnace cooled to 600°F. (b) 1275°F temper.
		0.23	1.35	0.30	0.011	0.020	0.21	0.20	0.64	–	–	
		0.20	1.31	0.25	0.012	0.023	0.20	0.17	0.47	–	–	
		(b) 0.22	1.33	0.30	0.017	0.013	0.21	0.12	0.52	–	–	
	T-1 (2-in.)	0.13	0.85	0.24	0.013	0.013	0.40	0.64	0.67	0.06	–	1700°F for 2 hr; water quenched; tempered 1150°F for 2 hr; retempered 1165°F for 2 hr, air cooled
Nickel Steels	A350-LF1 (Modified)	0.15	0.79	0.25	0.027	0.033	1.71	0.05	–	–	–	Normalized at 1600°F; water quenched; tempered at 1250°F; stress relieved at 1150°F
	A350-LF3 (3-5/8-in.)	0.14	0.52	0.25	0.031	0.032	3.28	0.04	0.05	0.04	–	
	HY-80 (3-in.)	0.14	0.21	0.19	0.011	0.014	2.91	1.55	0.54	0.04	0.06	1650°F for 3 hr; water quenched; tempered 1175°F for 3 hr; air cooled
	A353	0.10	0.47	0.29	0.008	0.023	8.9	0.06	0.15	–	–	Normalized at 1650°F, air cooled; renormalized at 1450°F, air cooled; tempered at 1050°F, air cooled

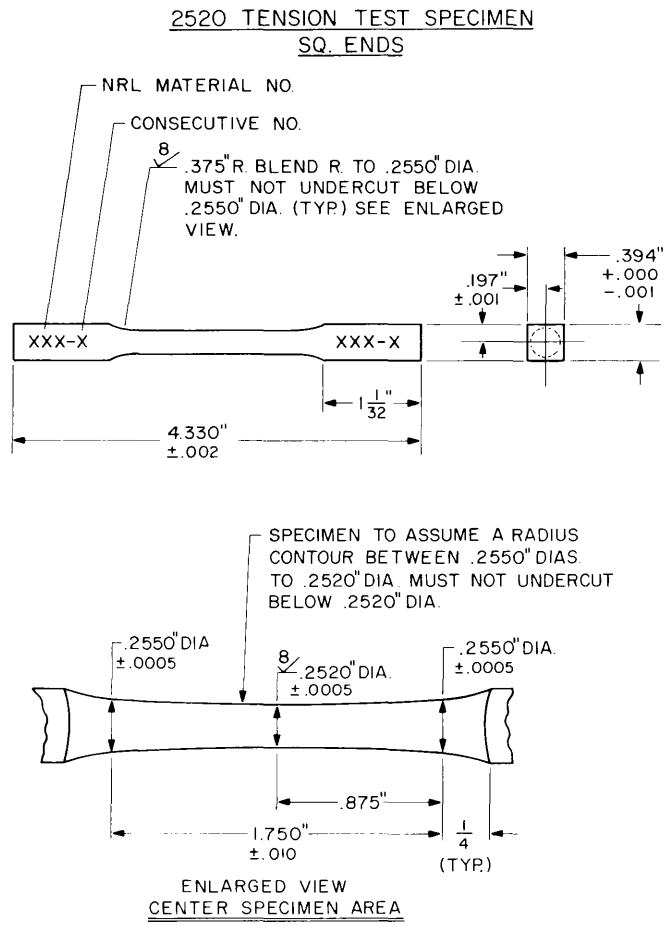

Fig. 1 - Details of the requirements for the recommended tensile specimen

The encapsulated specimens were irradiated in a number of different facilities at temperatures less than 250°F. The exposure levels* and irradiation temperatures for the several sets of specimens are presented in the summary tables in the Appendix. These specimens together with unirradiated reference specimens were than tested in the NRL hot cell facilities to determine the load-elongation curve to about 1% elongation and the load-minimum diameter curve from about 1% reduction of area to fracture. For a number of specimens, percent elongation was measured, although for the nontapered specimens, this measurement frequently was not possible. The reduction of area after fracture was usually measured, but only a limited number of measurements of uniform reduction of area were made.

From the two load-deformation curves recorded, the yield strength, tensile strength, percent elongation, percent reduction of area, maximum load strain, yield-to-tensile strength ratio, and true stress-natural strain relations for the individual tests were calculated.

*Dosimetry measurements have been discussed at length in other NRL Reports (12-15), and those interested in the procedures used are referenced to these earlier reports.

Metallography

Mechanical test specimen fragments as needed were sectioned for metallographic specimen preparation. Typical microstructures for the unirradiated steel conditions are reported in the next main section to provide suitable reference for the material tested.

Representation of the Test Data

Nominal stress-reduction of area summary plots have been used at length to report the tensile data. These curves, while readily established from the nominal load-change in diameter curves taken in the test, ideally should be converted to true stress-natural strain curves for use in combined stress systems. The curves plotted in true stress-natural strain coordinates are presented in the Appendix together with the ln true stress-ln natural strain curves which were used to establish the analytical form of the power series expressions which describe the stress-strain relations for the different steel conditions.

All numerical data that have been used in constructing the conventional properties-neutron flux curves throughout the report are accumulated in tables for the individual steels and are presented in the Appendix.

METALLOGRAPHIC STRUCTURES

The A212-B steel is a carbon-silicon steel with total alloy content including Mn and Si of about 1-1/2%. Consequently, it is a low hardenability steel, and for the 4-inch-thick section investigated the quenched and tempered structure consisted of equiaxed ferrite and fine pearlite, Fig. 2a. As shown in Fig. 3 the grain size of the steel was mixed and consisted of large pearlite clusters dispersed through a fine structure of ferrite and pearlite. This combination, in general, should possess somewhat inferior notch toughness.

Steel A302-B is a Mn-Mo steel of intermediate hardenability which does not readily form pearlite due to the significant Mo content. The typical bainitic structure found in this steel on quenching is retained throughout a 6-inch-plate section after tempering. The characteristic bainitic structure is presented in Fig. 2b.

Steel T-1 is a Ni-Cr-Mo-V steel with total alloy content of about 2-3/4%. The alloy combination employed in this steel gives it greater hardenability than that measured for the two steels already discussed. Increased hardenability together with the reduced plate thickness at which this steel was heat treated thus promoted the development of a fully martensitic structure on quenching. The tempered structure presented in Fig. 2c suggests that little if any high temperature transformation product was formed in this steel.

Steels which quench to variable microstructures from the surface to the center of the plate tend to lose the accompanying hardness differential on tempering. The hardness traverses for the A212-B, A302-B, and T-1 steel plates, given in Fig. 4, indicate this leveling of hardness especially well for the A302-B steel. This correlates with the uniform bainitic structure observed for this steel. For the other two steels there is a hardness minimum at the center of the plate.

A350-LF1 and A350-LF3 steels contain Ni additions in amounts sufficient to improve mechanical properties but which do not greatly increase hardenability. Because of a modest hardenability and low carbon content these steels during quenching transform to equiaxed ferrite and small clusters of fine pearlite. During tempering, the equiaxed ferrite for the most part is retained unchanged, while the carbide in the fine pearlite is agglomerated (Fig. 5a).

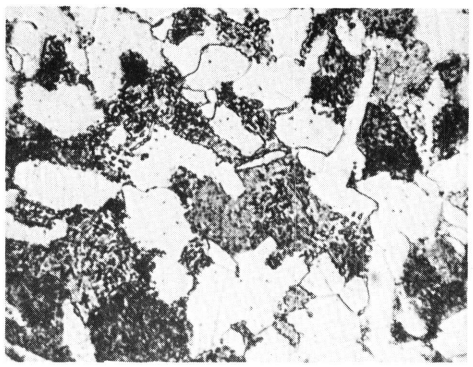

(a) A212-B

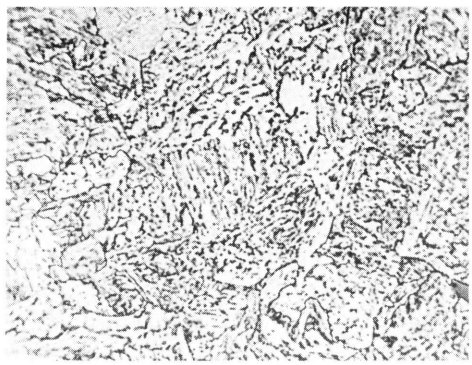

(b) A302-B

(c) T-1-1

Fig. 2 - Characteristic microstructures of the low nickel steels (1200X)

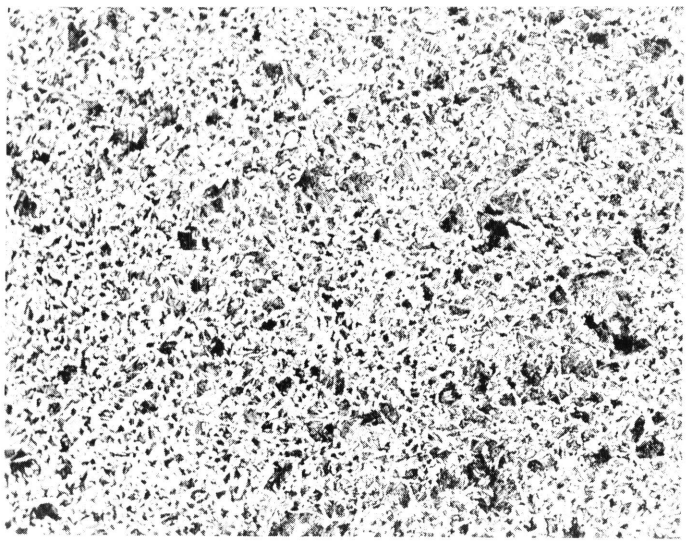

Fig. 3 - Mixed pearlite colony grain size whicl was typical for the A212-B steel (100X)

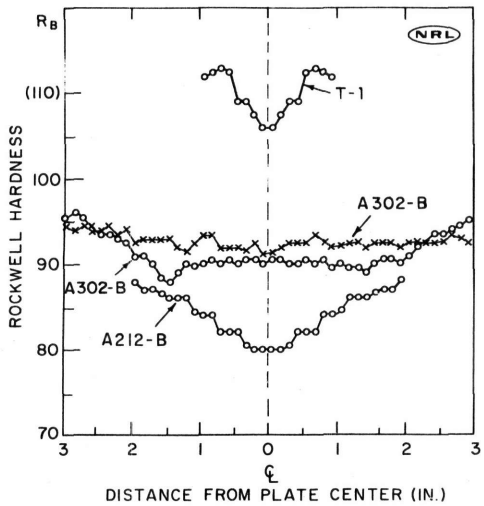

Fig. 4 - Through thickness hardness surveys of four low nickel containing steel plates

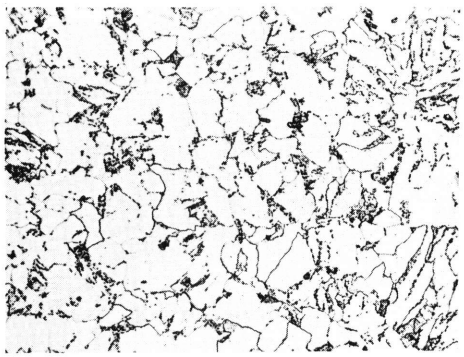

(a) A350-LF1 (500X)

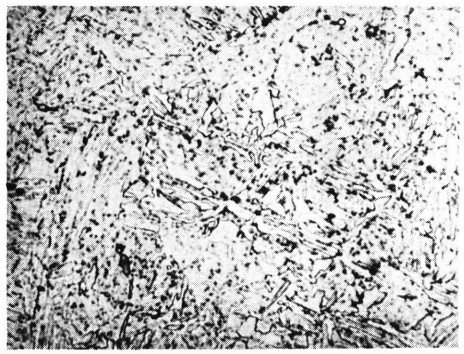

(b) HY-80 (1200X)

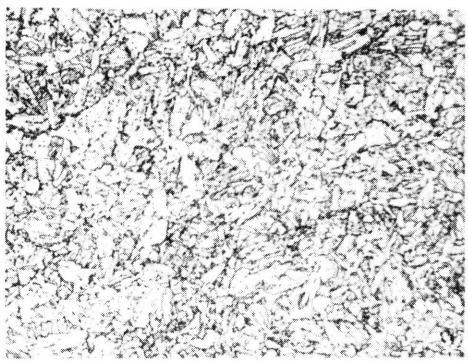

(c) A353 (600X)

Fig. 5 - Characteristic microstructures of the nickel bearing steels

HY-80 steel is a modified 43XX steel with Ni, Cr, and Mo contents increased, or it may be considered to be a 33XX-type steel modified with about 1/2% molybdenum. It is thus a steel with deep hardening characteristics, so that high temperature transformation products would not be expected even in relatively heavy sections after water quenching. On tempering, the carbides in the steel are precipitated and agglomerated while vestiges of the martensitic structure formed during quenching are retained (Fig. 5b).

A353 steel is an approximately 9% Ni steel with 0.15% Mo added. For the section thickness studied, the steel in the double normalized-tempered condition is effectively a tempered martensitic structure (Fig. 5c) which is extensively banded (Fig. 6).

The four nickel-bearing steels are of uniform hardness from surface-to-surface (Fig. 7), and the values correlate well with the microstructures observed for these steels.

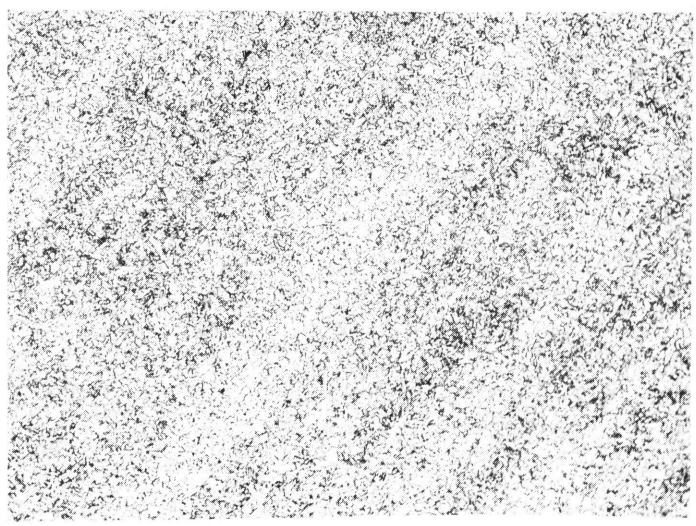

Fig. 6 - The banded structure observed for A353 steel (100X)

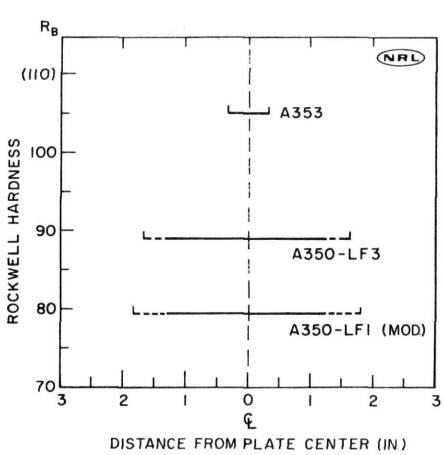

Fig. 7 - Through thickness hardness surveys of three nickel bearing steel plate and ring forgings

TENSILE PROPERTIES

The conventional properties of yield and tensile strength, elongation, and reduction of area were found to vary with changes in a number of factors. The more important of these factors are: (a) specimen orientation in the plate, (b) processing history of the plate, (c) chemical composition of the steel, and (d) integrated neutron fluence level.

Specimen Orientation

The nominal load-reduction of area curves for specimens oriented in the rolling, cross-roll, and thickness directions are presented in Fig. 8 for a 4-inch plate of A212-B steel. The number of tests completed for each specimen orientation is indicated in the figure.

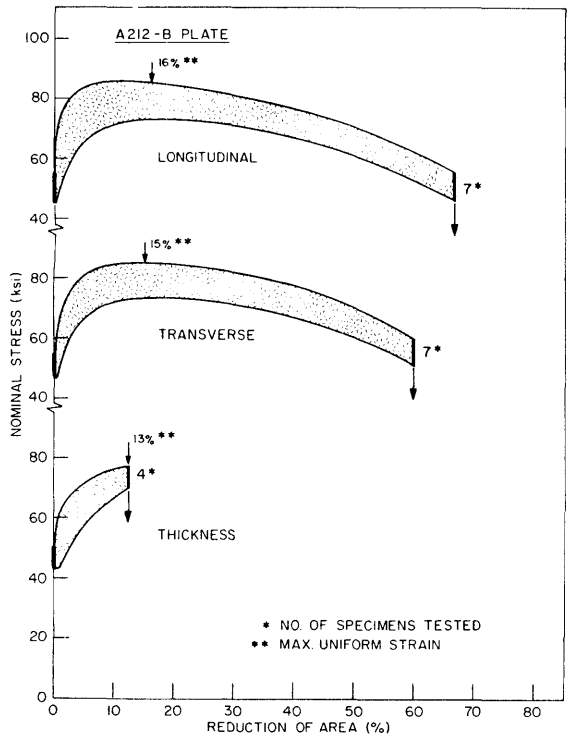

Fig. 8 - The nominal stress-reduction of area data bands for A212-B steel plate for the specimen orientations indicated

For this quenched and tempered steel, the yield strength for all specimen orientations was about 50 ksi or slightly less. The tensile strength was in excess of 80 ksi, with somewhat reduced values being measured with the thickness direction specimens. For these latter specimens, large nonmetallic inclusions were oriented normal to the length of the test section. With load application, these inclusions failed at low load, reducing the effective load-bearing cross section. While the consequent notch action due to inclusion failure tends to strengthen the test section, in general the inclusions were of such size that their failure led to nominal load reduction.

The elongation and reduction of area were of maximum values in the rolling direction and only slightly reduced in the cross-roll direction.

Nominal strength-reduction of area curves for the three principal plate directions for a 6-inch-thick plate of A302-B steel are presented in Fig. 9. The yield strength was about 65 ksi, and the tensile strength approximated 90 ksi. The ductility was a maximum in the rolling direction with a reduction of area of 65% and elongation of 30%. Ductility was slightly reduced in the cross-roll direction and was a minimum in the thickness direction, where the reduction of area was about one-fourth of that measured in the rolling direction.

Processing History

All steels are subject to variable mechanical processing history both in the steel mill and in fabricating a structure. This may lead to significantly variable strengths in

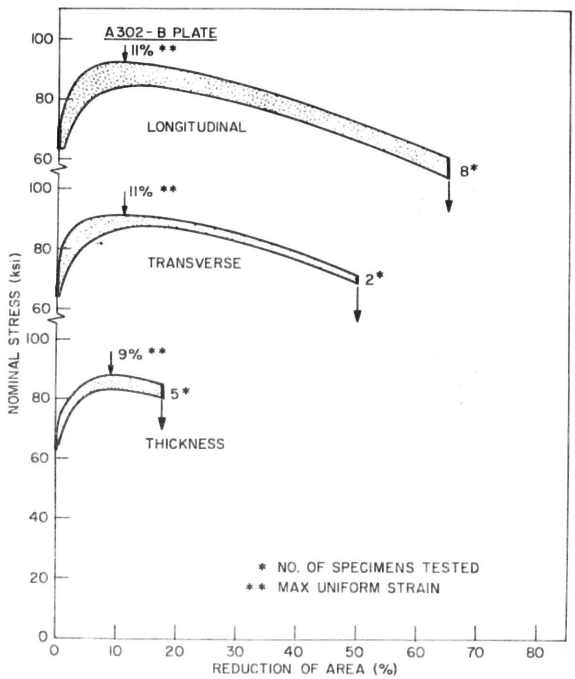

Fig. 9 - The nominal stress-reduction of area data bands for A302-B steel plate for the specimen orientations indicated

different portions of a structure as is suggested by the nominal stress-reduction of area curves for A350-LF1 steel presented in Fig. 10.

The conventional yield strengths (not shown) of the two lots of steel from the same heat differ by about 10%, the minimum being about 46 ksi as compared with the maximum of about 54 ksi. The minimum tensile strength was 64.5 ksi compared to the maximum of about 77 ksi. This variability of nearly ±10% in the tensile strength is large compared to that expected for bar stock but may be considered as not unusual for plate.

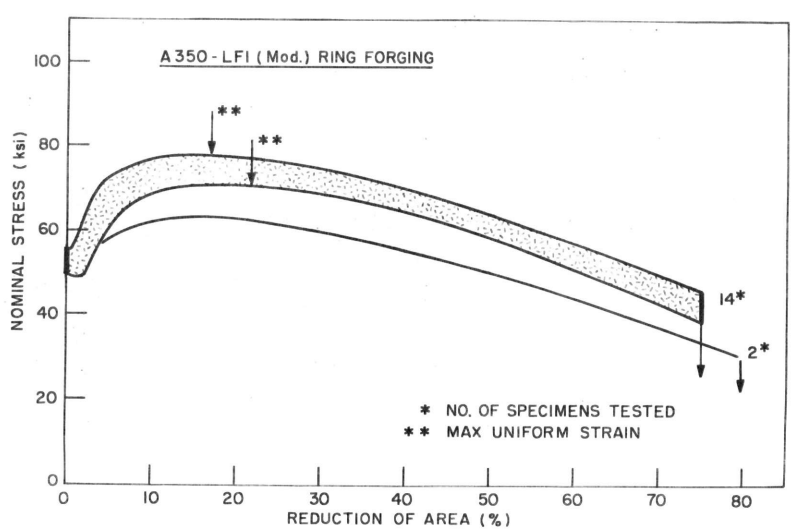

Fig. 10 - The nominal stress-reduction of area data bands for two lots of the same heat of A350-LF1 (Modified) steel

Steel Composition

The strength properties of a given steel are determined by its metallurgical structure, which is governed by its heat treatment. For a given metallurgical structure the strength of a steel is variable within limits as a function of alloy content. In thick plate, processing leads to alloy segregation through the plate, and this segregation influences the strength by altering the metallurgical structure, by changing the hardenability of the steel and by a solution hardening effect. The solution hardening cannot, in practice, be eliminated, but extreme structural differences due to hardenability differences can be eliminated by prolonged tempering at the maximum permissible temperatures. However, because of the wide range in alloy content for the steel studied, relatively large differences in strengths are possible. This is illustrated by the nominal strength-reduction of area curves presented in Fig. 11 for low-nickel steels and in Fig. 12 for nickel-bearing steels.

For the A212-B steel, the results for 32 tension tests are encompassed within the maximum and minimum envelopes (Fig. 11). For this quenched and tempered steel, the ranges of the conventional tensile properties are given in Table 2.

For the A302-B steel, the maximum and minimum envelopes also encompass the results of 32 tension tests. The ranges of the nominal tensile properties for this steel and for 0.40% Ni T-1 steel are also listed in Table 2.

The range of strengths in the medium to high nickel steels is from a minimum of 64 ksi to a maximum of 115 ksi or about the same as that for the low nickel steels, and the nominal strength-reduction of area curves are summarized in Fig. 12. The ductilities of these steels as determined by the percent reduction of area are higher than those

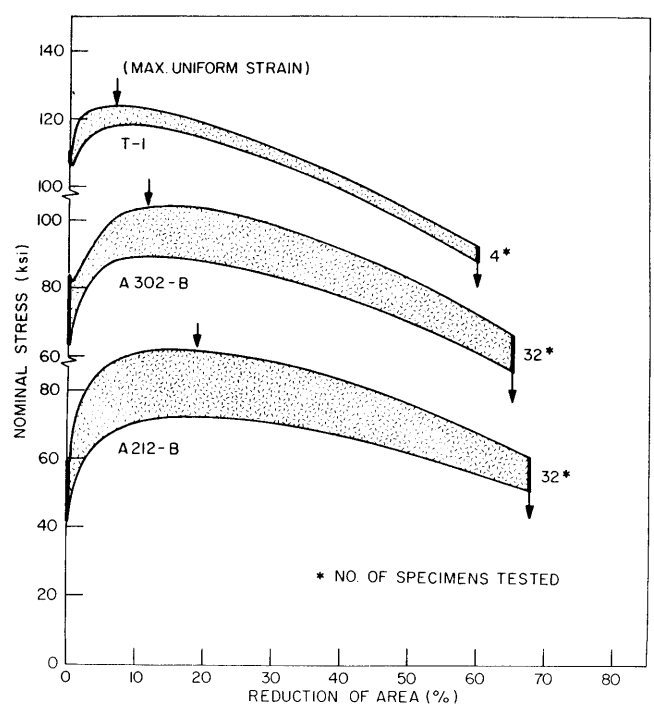

Fig. 11 - Nominal stress-reduction of area data bands for the three low nickel steels in the unirradiated condition

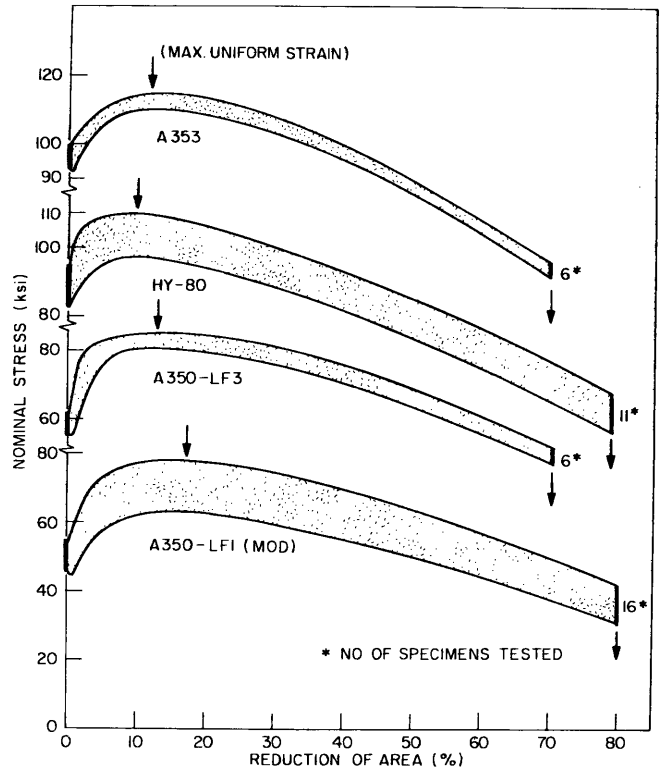

Fig. 12 - Nominal stress-reduction of area data bands for four nickel bearing steels in the unirradiated condition

Table 2
Tensile Properties for the Steels in the Unirradiated Conditions

Type of Steel	Yield Strength (ksi)		Tensile Strength (ksi)		Reduction of Area (%)		Elongation (% in 1-in. gage length)	
	Min.	Max.	Min.	Max.	Min.	Max.	Min.	Max.
A212-B	41.25	58.6	72.75	92.8	54.5	67.0	30.6	40.0
A302-B	63.8	83.5	84.5	104.0	54.5	67.0	22.3	32.6
T-1	107.7	—	118.0	—	64.0	—	19.0	—
A350-LF1 (Modified)	46.25	54.8	64.3	77.15	61.0	80.0	34.5	40.0
A350-LF3	56.0	60.2	80.75	84.0	69.5	72.0	32.0	35.0
HY-80	82.1	94.0	96.3	109.25	73.5	78.5	21.0	31.0
A353	92.6	99.75	109.5	114.25	68.5	69.0	28.5	32.0

measured for the preceding series of steels. The conventional tensile properties are summarized in Table 2 for comparison.

The conventional tensile properties for all the steels before irradiation are summarized in Fig. 13, where from left to right the steels are arranged in order of decreasing tensile strength. The yield strength is largely determined by the tensile strength; the yield strength-to-tensile strength ratio is about 0.90 at the maximum strength level. This ratio decreases to 0.60 for the low nickel steels and to 0.70 to 0.75 for the nickel-bearing steels at the minimum strength levels.

The strain at maximum load, which is determined from the reduction in cross section at maximum load, is a minimum at the highest strength levels and approximates a value of 0.1, which corresponds to about 10% elongation. This quantity increases with reduction in tensile strength to nearly 0.2, which corresponds to a uniform elongation of about 17%.

The tensile test properties considered to this point follow the same trend lines for the two sets of steels. However, the ductilities for the two groups of steels as indicated by the reduction of area differ with that for the nickel-bearing steels, being about 15% greater than that measured for the low nickel steels.

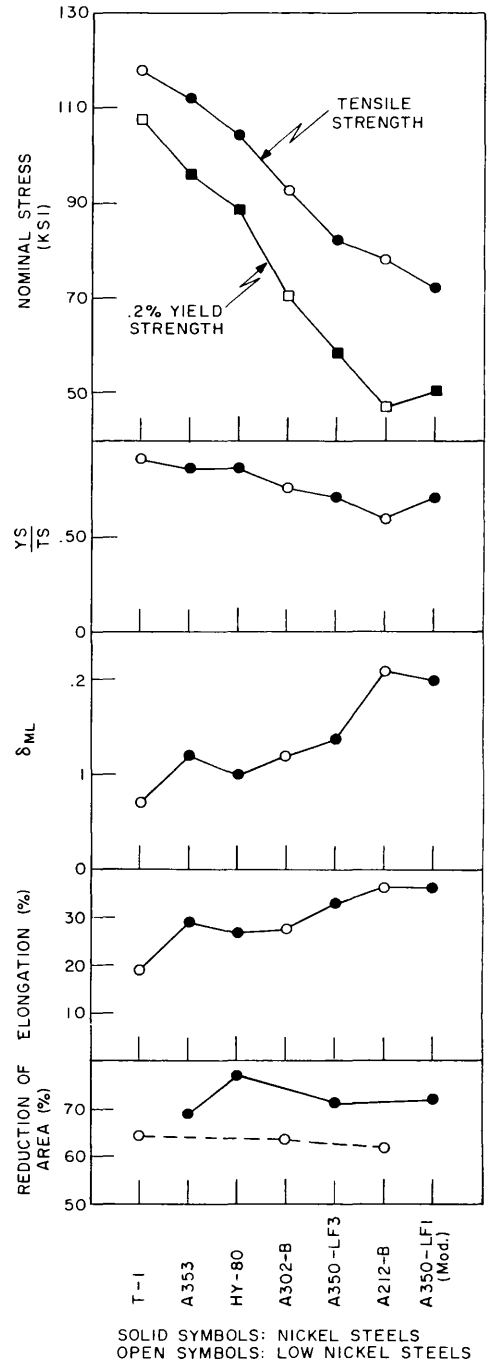

Fig. 13 - The conventional tensile properties of the seven steels in the unirradiated condition

Neutron Fluence Exposure

With exposure in an environment containing a significant number of fast (>1 Mev) neutrons,* a steel undergoes tensile properties changes as indicated by the nominal strength-reduction of area curves in Fig. 14 for A212-B steel. As the fast neutron fluence increases, for an irradiation temperature less than 250°F, the yield strength is increased and at a fluence level of about 10^{19} n/cm^2 becomes equal to the tensile strength. With further exposure to neutrons, the maximum nominal load is measured at the yield strength strain, so the yield strength also determines the tensile strength.

When the yield strength becomes equal to the tensile strength, the maximum load strain passes from the value of 0.1 to 0.2 measured for the unirradiated material to values about equal to those at which the yield strength is measured. This corresponds in a structure to a change in ductility before collapse from 10 to 15% elongation to a value of about 0.1 to 0.2%

*Fast neutron fluence values given in this report are based on the assumption of a fission spectrum distribution of neutrons

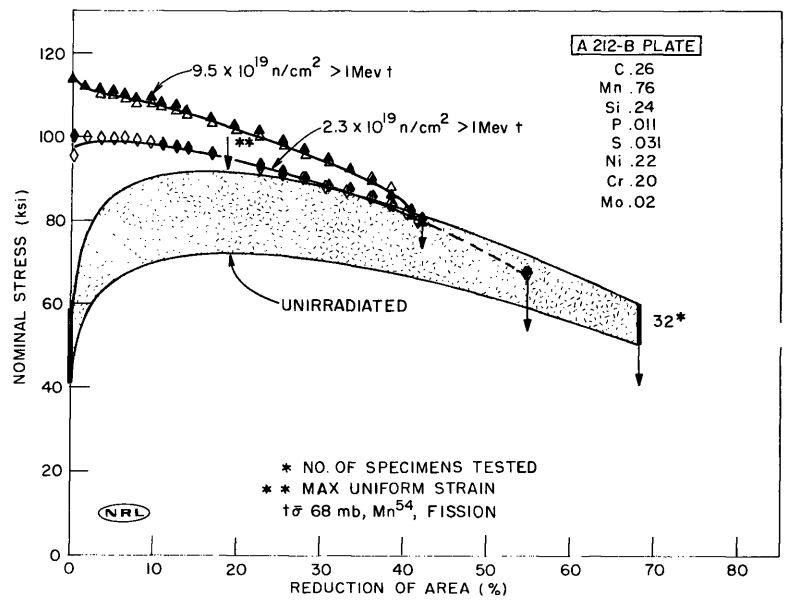

Fig. 14 - Comparative nominal stress-reduction of area curves for A212-B steel after indicated neutron radiation exposures at <250°F

The reduction in uniform elongation or general deformation in a structure, however, may not be associated with a severe lowering of the reduction of area, which is the local strain in the vicinity of the fracture, as is illustrated in Figs. 14, 15, and 16. For each of these steels, the uniform elongation after a fast neutron fluence of 9.5×10^{19} n/cm^2 is of the order of 0.2% but the reduction of area is measured at over 40%, which compares favorably with the maximum observed value of about 65%.

For certain of the quench and temper steels, notably those containing medium and high nickel contents, a fast neutron fluence of 9.5×10^{19} n/cm^2 leads not only to reduced uniform elongation but also to a loss of ductility as registered by the reduction of area. Thus for the four steels yielding the nominal strength-reduction of area curves in Figs. 17 through 20, the reduction of area after exposure to a neutron fluence of 9.5×10^{19} n/cm^2 falls in the interval of 10 to 20%. The average value of 15% is only one-quarter the value registered for the unirradiated steels.

The conventional tensile properties of the steels are summarized in Figs. 21 and 22, where the numerical magnitudes of the tensile properties are plotted, and in Fig. 23, where the percentage variations in these quantities are presented. The tensile and yield strengths increase with increased exposure at numerical rates that are uniform for the various steels regardless of composition or strength level. The reductions of area for the nickel-bearing steels, however, are clearly much reduced compared to those for the low-nickel steels.

The manner in which the tensile properties of the various steels changes with neutron fluence level is better shown by plotting the respective numerical values against fluence level with material as the parameter (Figs. 24 and 25). At an exposure level of 10^{19} n/cm^2, the yield and tensile strengths are nearly equal, while at greater exposures the tensile strength is measured at the yield strength strain. At exposure levels less than 10^{19} n/cm^2 the tensile and yield strengths diverge to become equal to the characteristic values measured for the unirradiated steel conditions.

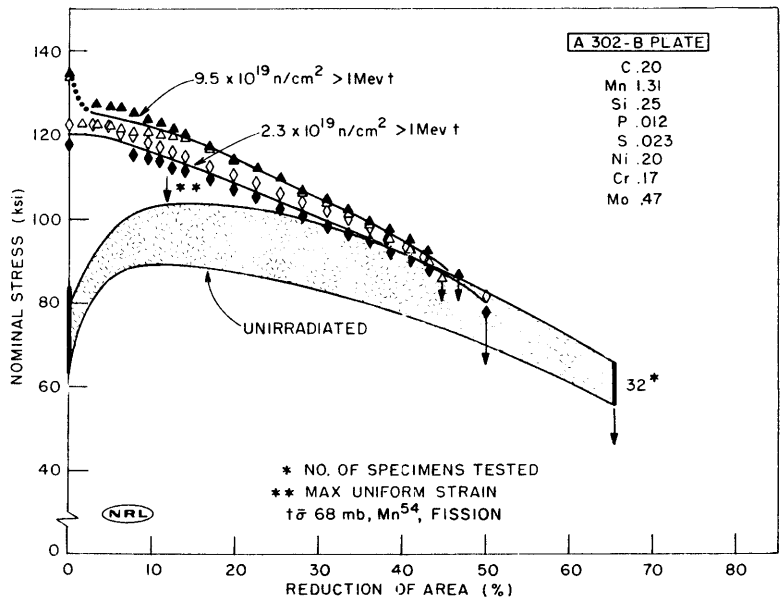

Fig. 15 - Comparative nominal stress-reduction of area curves for A302-B steel after indicated neutron radiation exposures at <250°F

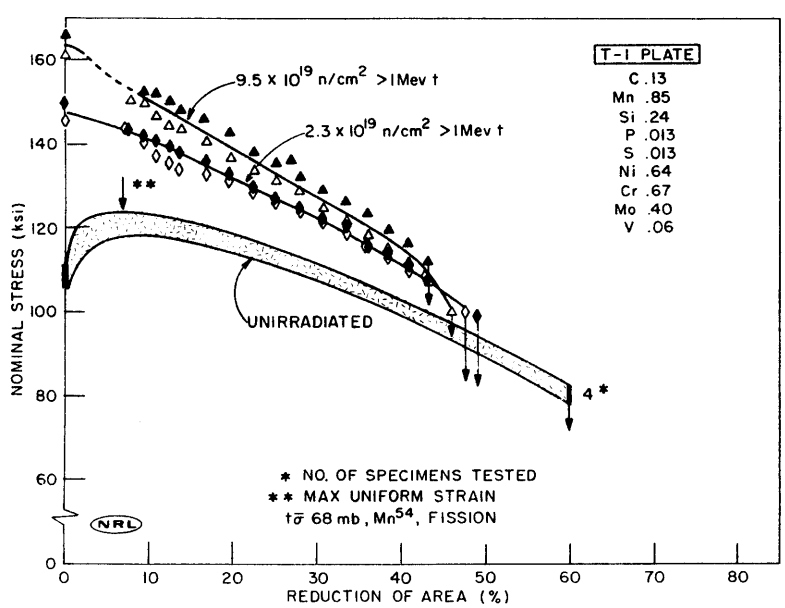

Fig. 16 - Comparative nominal stress-reduction of area curves for T-1 steel after indicated neutron radiation exposures at < 250°F

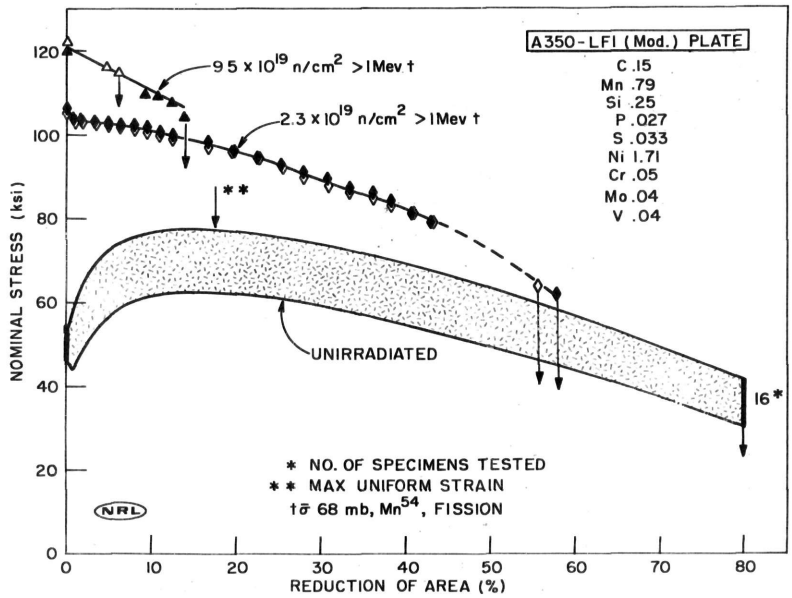

Fig. 17 - Comparative nominal stress-reduction of area curves for A350-LF1 steel after indicated neutron radiation exposures at < 250°F

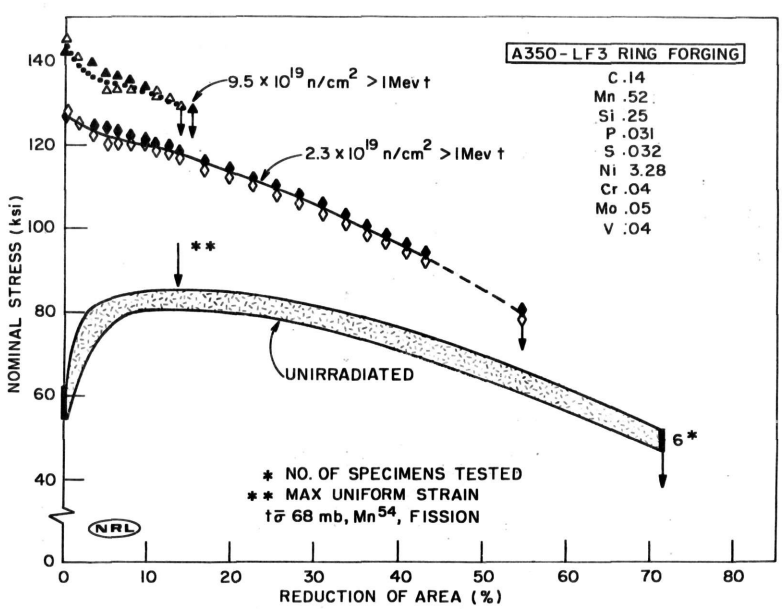

Fig. 18 - Comparative nominal stress-reduction of area curves for A350-LF3 steel after indicated neutron radiation exposures at < 250°F

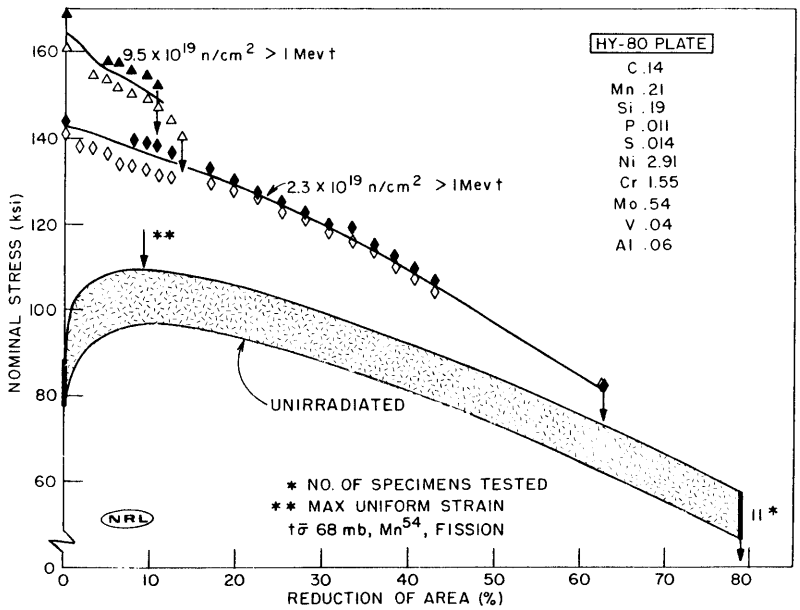

Fig. 19 - Comparative nominal stress-reduction of area curves for HY-80 steel after indicated neutron radiation exposures at < 250°F

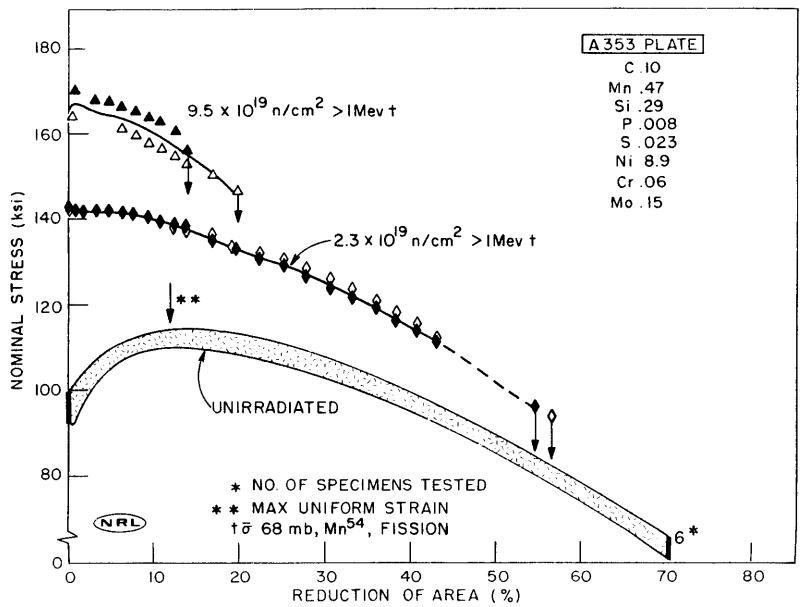

Fig. 20 - Comparative nominal stress-reduction of area curves for A353 steel after indicated neutron radiation exposures at < 250°F

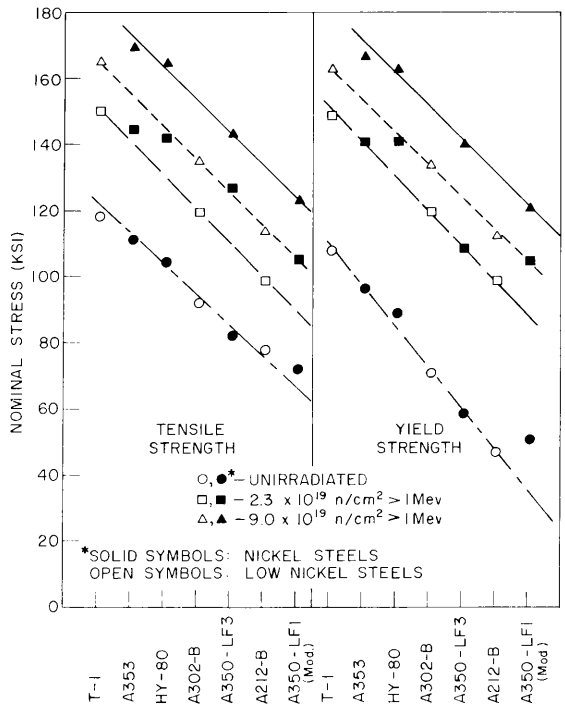

Fig. 21 - The tensile and yield strengths for the seven steels after neutron radiation at < 250°F to the fluence levels indicated

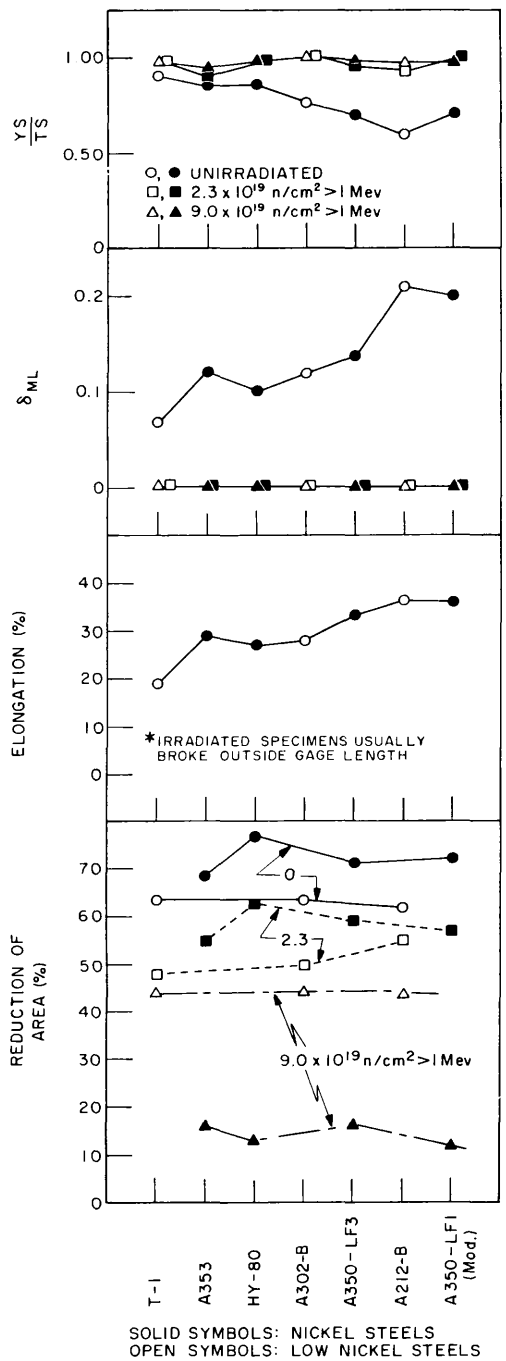

Fig. 22 - Additional strength and ductility properties for the seven steels after neutron radiation at < 250°F to the indicated fluence levels

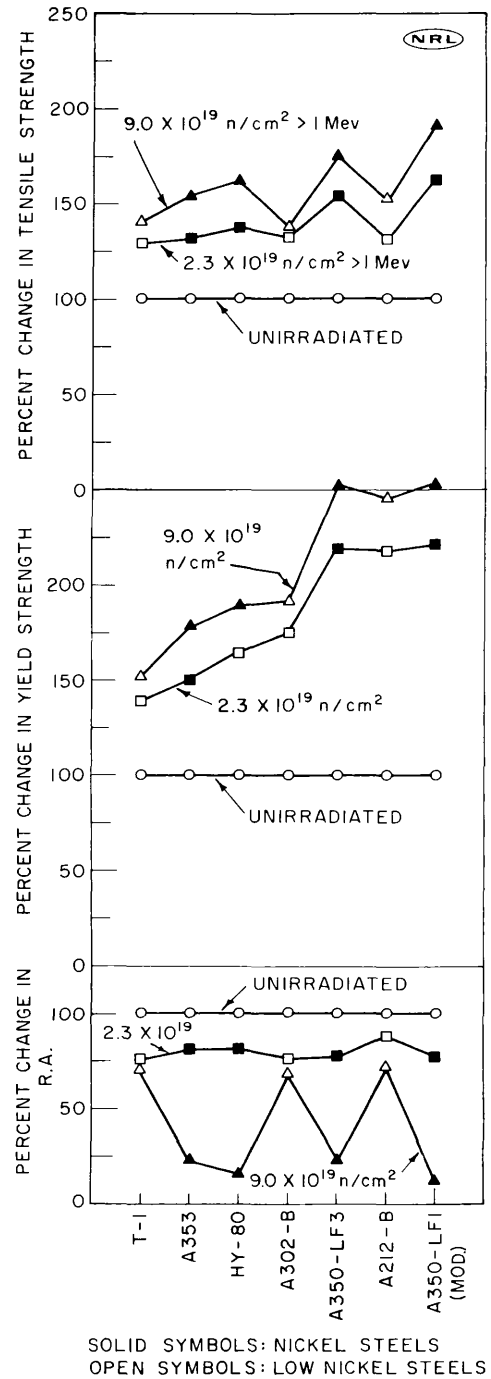

Fig. 23 - The percent change in the tensile and yield strengths and reduction of area with indicated neutron exposures at < 250°F

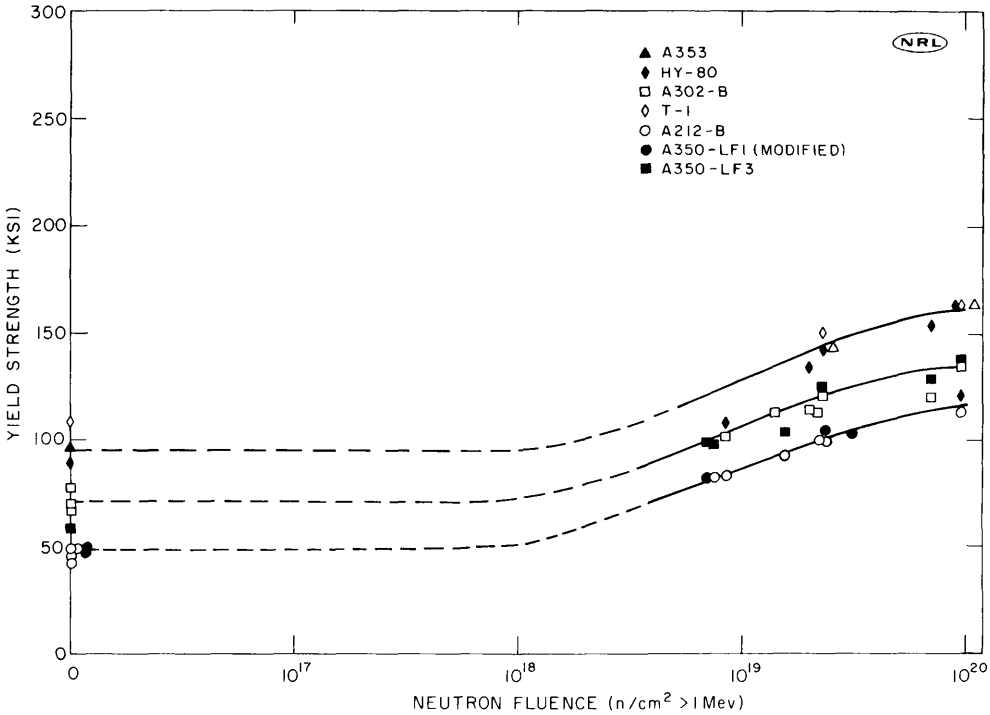

Fig. 24 - The yield strengths of the seven steels as a function of neutron fluence at < 250°F

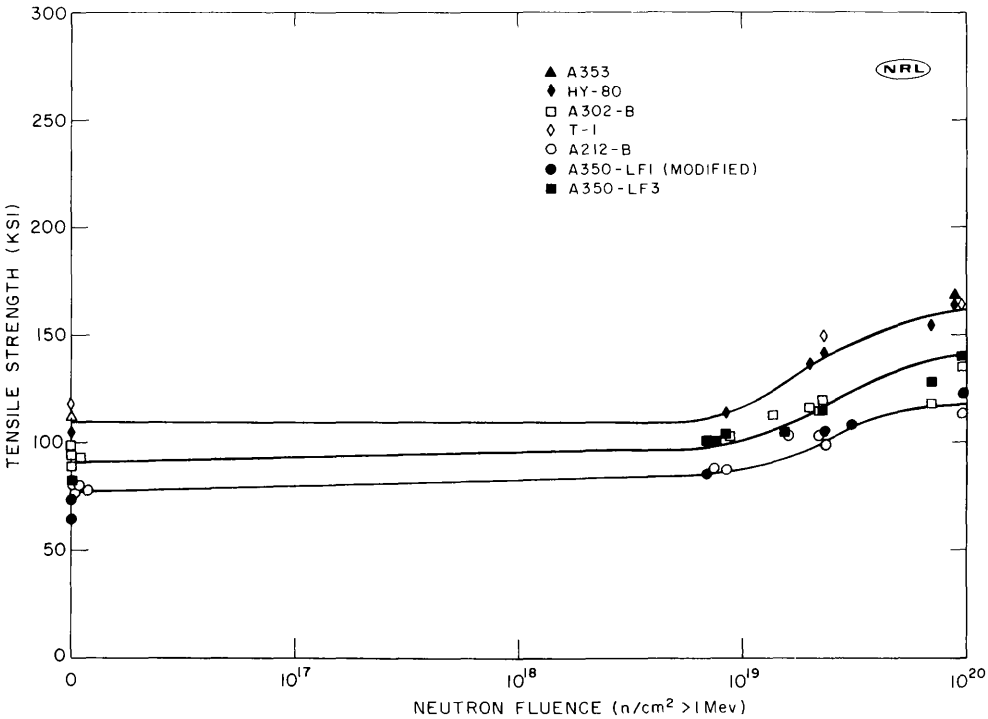

Fig. 25 - The tensile strengths of the seven steels as modified by neutron exposure at <250°F

The conventional indexes of ductility measured in the tension test are percent reduction of area and percent elongation. These values taken for the present series of steels are summarized in Figs. 26 and 27. Preliminary inspection of these two sets of data, both of which generate transition type curves, suggest a significant disparity in level of fluence at which the ductility transitions occur.

The reduction of area curves, which are usually considered to provide the more meaningful index of ductility, show ductile-brittle transitions that depend on the nickel content of the steels, but for all steels this ductility transition occurs at exposure levels in excess of 5×10^{19} n/cm^2 (Fig. 26). The indicated transition as measured by elongation, on the other hand, is well developed at a neutron fluence level of 1.0×10^{19} n/cm^2

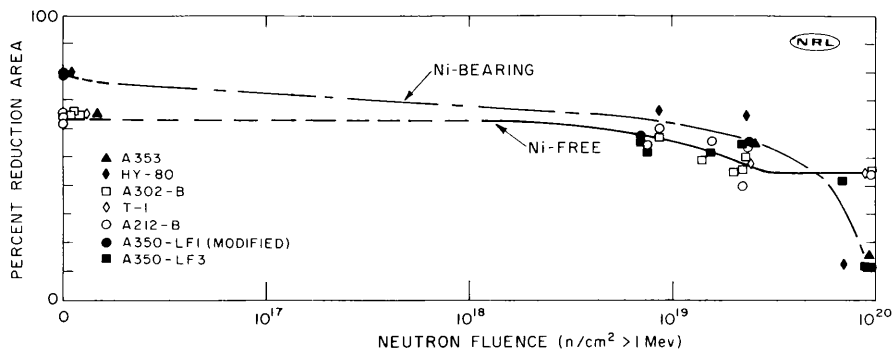

Fig. 26 - The reduction of area of the seven steels as a function of neutron fluence at < 250°F

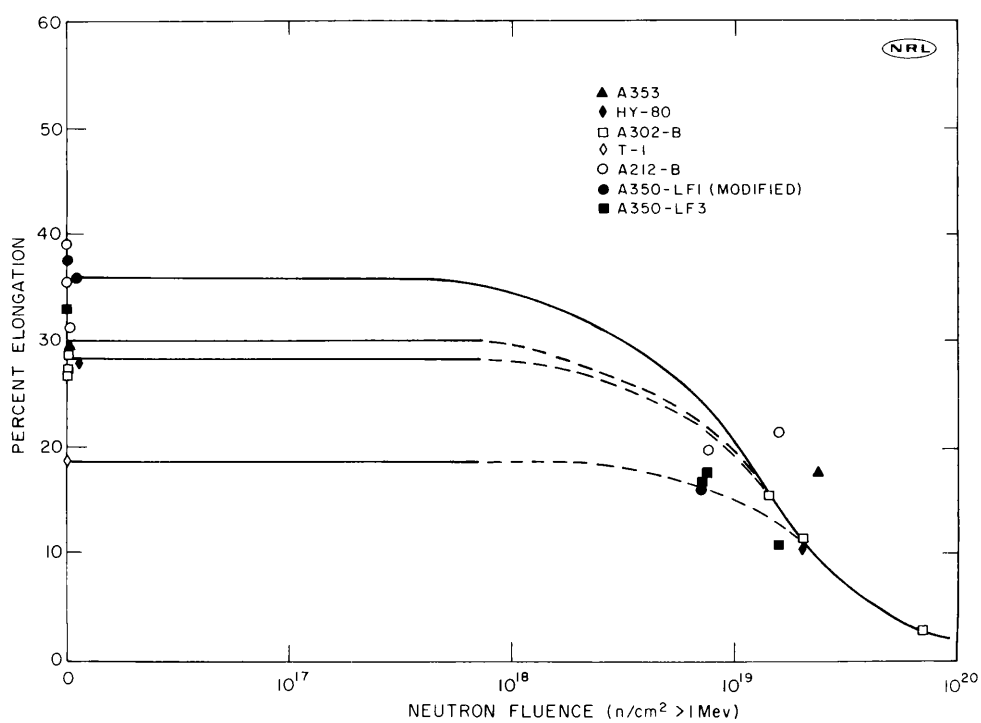

Fig. 27 - The elongations of the seven steels as a function of neutron fluence at < 250°F

(Fig. 27). This is potentially a 500% life prediction differential, and this difference must eventually be evaluated as to its meaning with reference to service performance. The mechanical factors which produce this behavior, however, are straightforward and relate to the instability strains that are measured as function of neutron exposure. These instability strains, as measured both with reference to the maximum load strain determined from the autographic stress-strain curves and with reference to the deformation away from the necked section in the tension specimen, are presented in Fig. 28. From these curves ductile-brittle transitions as determined from gross deformation capabilities of a structure are completed for the more radiation-sensitive materials at exposure levels of about 10^{19} n/cm^2 and for the less sensitive materials by exposure levels of 5×10^{19} n/cm^2. The instability strain data, then, correlate with the percent elongation data. These data, in turn, correlate directly with the deformation to failure capabilities of the structure. Thus, for neutron exposure levels in excess of 1 to 5×10^{19} n/cm^2 at less than 250°F, the deformation energy required to break a structure constructed of martensitic steels can be expected to be much less than that normally observed for steels with either high or low ductility as determined by reduction of area.

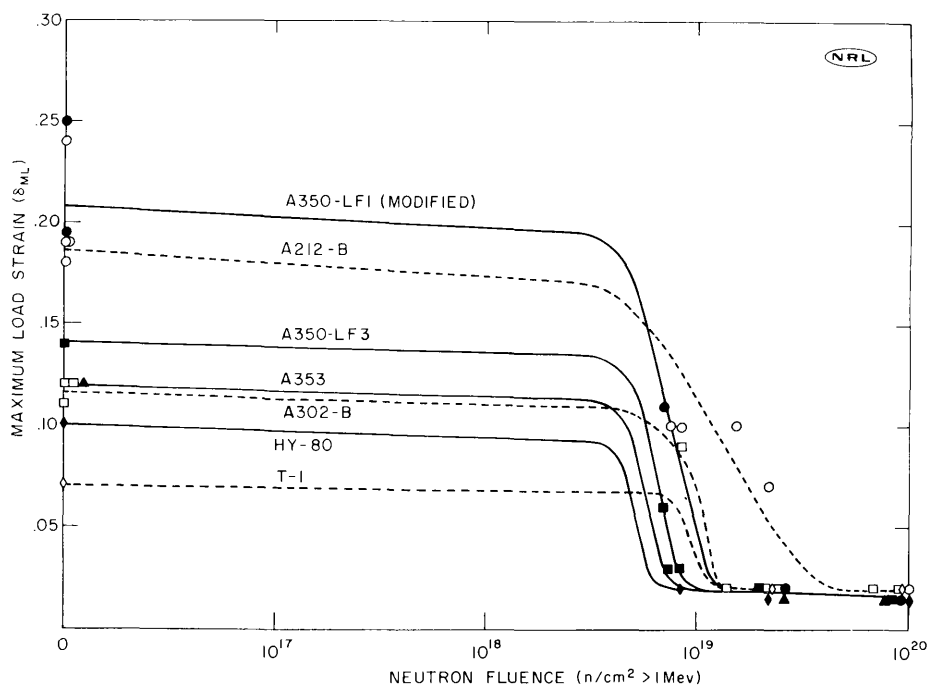

Fig. 28 - The maximum load strains of the steels as a function of neutron fluence at < 250°F

Tensile Specimen Fractures

All tensile specimens for the unirradiated and low level irradiation conditions failed with the conventional cup-cone type fracture surfaces. For the specimens exposed to neutron fluences approximating 9.5×10^{19} n/cm^2 those in the low nickel category developed percent reduction of areas of about 40%, which is sufficient to require the development of a pronounced necked-down section. Such specimens tended to develop cup-cone fractures (Fig. 29). The cup segments of these fractures, however, usually were not well formed and frequently showed 45-degree tears. These 45-degree-tear fractures were also suggested in the flat fractures which formed the top elements of the conical portions of the fractures.

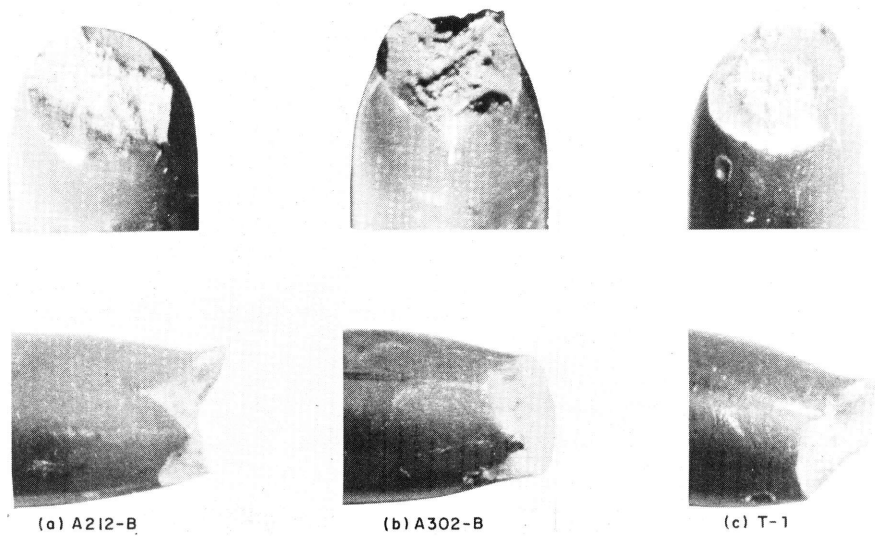

Fig. 29 - High ductility tensile fractures for the indicated steels after neutron exposure of 9×10^{19} n/cm^2 at < 250°F

The low ductility fractures obtained for certain of the specimens at the exposure level of 9.5×10^{19} n/cm^2 were frequently flat and brittle appearing as in Fig. 30a. These specimens also formed low ductility cup-cone type fractures as given in Fig. 30b and look much like the low ductility fractures obtained for hydrogen embrittled high strength steels. The absence of large ductility for these fractures is indicated by the two fracture orientations presented in Fig. 30c.

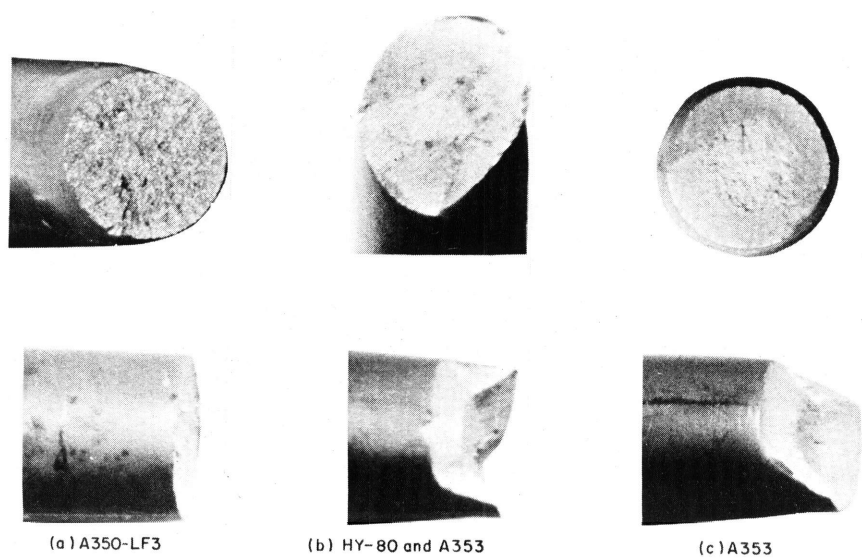

Fig. 30 - Low ductility tensile fractures for the indicated steels after a neutron exposure of 9×10^{19} n/cm^2 at < 250°F

DISCUSSION OF RESULTS

The conventional stress-strain relations for the steels have been treated at length in presentation, and it is evident that the conventional numerical data frequently do not adequately establish the behavior to be expected in structural applications when the steel is exposed in service to neutron radiation. This is particularly true of the ductility to be expected at ambient temperatures when this is reported as percent reduction of area and percent elongation as conventionally measured. By these two criteria all steels studied possess significant ductility for neutron exposures in excess of 10^{19} n/cm^2; but for the indexes of instability strain, appreciable general ductility at these fluence levels for low exposure temperatures is not to be expected.

Supporting data for this deduction from applications in combined stress environments are the tube test results reported by Trozera and Flynn (6) and the numerous fracture test results that are reported in the literature (11,16-21). However, the fracture toughness data are not amenable to the quantitative correlation with tensile data that is possible with the tube tests, where the correlation, while not exact, is deemed adequate. However, on the basis of energy to cause fracture as determined by gross deformation, the tensile and tube tests are in excellent qualitative agreement. These tests suggest that after a neutron irradiation exposure sufficient to lower the uniform strain to about the yield strength strain the relative energy absorbed in fracturing a structure rapidly drops as the size of the structure increases regardless of the local strain at the fracture surface. This behavior corresponds to the generally recognized fall-off in percent elongation measurements as the gage length of a tensile specimen is allowed to increase. For the irradiated steels the strain value that is approached in the structure at collapse is the yield strength strain. However, as was first shown by Ludwik (22) this instability strain must be suitably converted first into generalized strain. Adequate approximations of such generalized strain are provided by the logarithmic or natural strains when the plastic strain contribution is large compared to the elastic strain and when isotropy in the deforming material is assumed. However, both of these factors deviate from ideal behavior, and these deviations are known to lead to large percentage errors under certain conditions of application of the conversion procedure. In addition these errors are important despite the possibly small total strain value that one obtains in radiation-damaged steels. Of the two sources of error the assumed isotropy factor is the more difficult to evaluate, and it can lead to a larger error than that due to uncompensated elastic strain. In addition, at the very low instability strains that may characterize radiation-damaged steels, both factors are additive and should be compensated if the disagreement between measured and predicted instability strain is to be minimized.

The instability strain data reported in this report are not compensated for these two sources of error, as there is no generally accepted procedure to effect this adjustment. This, however, should cause no serious difficulty in the use of the data, which are presented in sufficiently expanded form to allow adjustments for these two factors as may be deemed prudent.

The plastic yielding conditions for a cylindrical tension specimen with circumferential fatigue crack have been described by Hill (23) who gives the value of the notch strength (σ_N) for this specimen in terms of the yield strength as

$$\sigma_N = 2.57K = \frac{2.57}{\sqrt{3}}\sigma_{ys} = 1.484\sigma_{ys}$$

The values of σ_N obtained in this manner provide the means to calculate the fracture toughness index K_{Ic}. However, this calculation of K_{Ic} requires an assumed plastic zone size at the notch base which is difficult to establish for steels in the strength range under study. The values of σ_N for the different steels as calculated are presented in Fig. 31. Experimental data are not available at this time to allow further discussion of these notch strength trends.

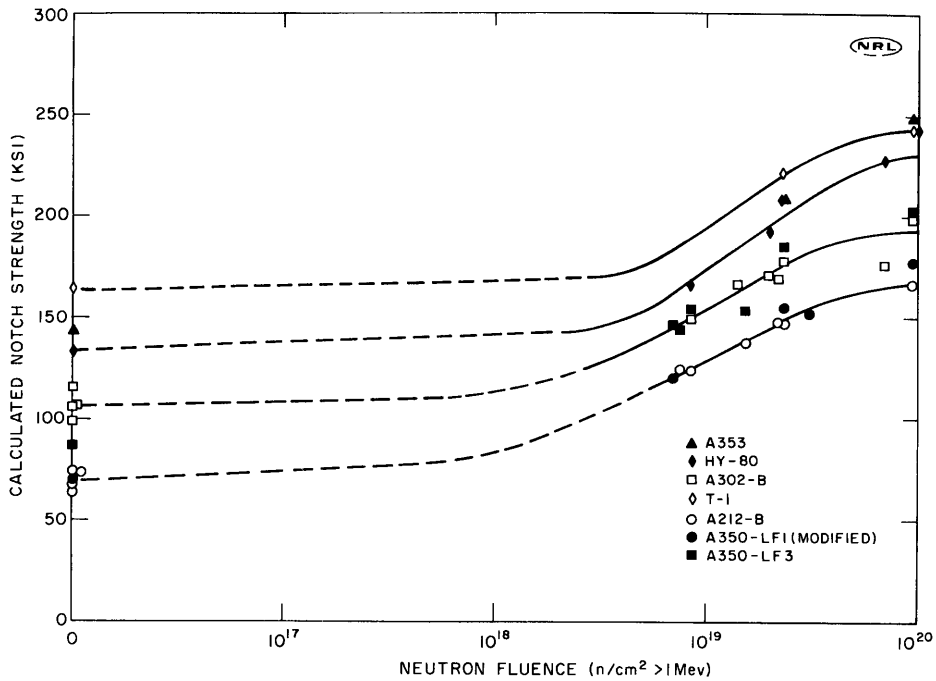

Fig. 31 - The notch strength for a cylindrical specimen with a circumferential fatigue crack as calculated for σ_N = 2.57K

It has already been stated that the nominal stress-strain properties of a steel must be stated in generalized stress-strain coordinates to be applicable in systems of multiaxial stresses such as the stress system in a reactor pressure vessel. In addition, it has been indicated that the true stress-natural strain representation is a suitable generalized coordinate system for this purpose. The natural strain coordinate is nearly linearly related to the percent reduction of area at low strains, but at the maximum strains attained in the tension test this linearity ceases to exist. The true stress and nominal stress values are nearly equal near the yield strength strain but diverge with increasing strain to differ by 10 to 15% at maximum load strain. At still greater strains the two stress representations deviate sharply, with the true stress progressively increasing and the nominal stress progressively decreasing.

The stress-strain data converted to the true stress-natural strain coordinate system, however, are still nominally presented in graphical form, and it is desirable to express these data in an adequate yet simple analytical form. This can be done by suitable use of a power series expression employed initially by Ludwik (22) and more recently by Hollomon (24) and Low (25).

The analytical expression in its more simple form as proposed by Holloman is

$$\sigma = \sigma_0 \delta^n,$$

where σ is the true stress, σ_0 is the strength coefficient (σ at $\delta = 1$), δ is the natural strain, and n is the strain hardening exponent. In this form the steel is treated as deforming plastically with initial load application, and the curve developed from the equation is initiated at the stress-strain coordinate origin. The natural strain at maximum load equals the strain hardening exponent, $\delta_{ML} = n$. For steels with yield strengths at about 50% of the tensile strength, the calculated curve obtained with this expression

approximates well the stress-strain curve measured when the latter is plotted in true stress-natural strain coordinates. For low strength steels, therefore, simple application of the above expression after specification of the yield strength and fracture strain allows the stress-strain curve either in conventional or true stress-natural strain coordinates to be faithfully plotted. However, as the yield strength increases relative to the tensile strength, the yield strength contribution to the stress-strain curve can no longer be ignored but must be superimposed on the work hardening curve that may be considered as characteristic for the steel. This portion of the stress-strain curve again is established by a power series expression such as that given above but for which the numerical value of n, the strain hardening exponent, is very small. Therefore, as the yield strength steadily increases to exceed the conventional tensile strength, the instability strain, which corresponds to the maximum load strain, may discontinuously change to a value reduced by one to two orders of magnitude. This change is established by the condition

$$\sigma_{0,(Y.S.)}\,\delta^{n(Y.S.)} > \sigma_{0(T.S.)}\,\delta^{n(T.S.)}$$

For convenience the following notation will be used:

$$\sigma_{0,(Y.S.)} = \sigma_{0,1}$$

$$\sigma_{0,(T.S.)} = \sigma_{0,2}$$

$$n_{Y.S.} = n_1$$

$$n_{T.S.} = n_2 .$$

For the radiation-damaged steels the flow stress at low strains may maximize sensibly at the strain value corresponding to n_1. If the steel does not break at this point, the stress does not fall abruptly as would be expected, but rather the drop-off in the flow stress is reduced and corresponds to the condition specified by the parameters ($\sigma_{0,2}$; n_2). For this reason the flow curve to maximum load corresponds to the value predicted from

$$\sigma = \sigma_{0,1}\,\delta^{n_1} \quad \text{(to maximum load)} \tag{1}$$

but the flow curve at large continuing strains corresponds to the value predicted from

$$\sigma = \sigma_{0,2}\,\delta^{n_2} \quad \text{(large strains to fracture)} \tag{2}$$

At the conventional strain rates employed in tension testing the flow curve between the strains corresponding to n_1 and n_2 is not well defined but depends on the strain rate. However, the curve is reasonably approximated by a straight line tangent to the two calculated curves that are developed in conventional nominal stress-strain coordinates through use of the two characteristic equations. In this way, again, the conventional stress-strain curves can be well approximated from the analytical expressions. The appropriate numerical equations for each set of curves are entered on the true stress-natural strain figures that are contained in the Appendix.

SUMMARY

The conventional tensile properties for selected irradiated conditions of seven steels of interest for possible use as constructional materials for reactor containment vessels have been determined at an ambient temperature of 75 °F. In addition, the load-elongation curves to a nominal 1% elongation and the load-diameter curves from about 1% reduction of area to fracture have been recorded. Limited hardness, metallographic, and fractographic data have also been presented. The following points are emphasized.

1. The steels studied are ferritic steels but are further subdivided into pearlitic, bainitic, and martensitic classes; representative microstructures of each steel are given (Figs. 2, 3, 5, and 6). Three of the steels are low nickel steels, and four are medium to high nickel steels.

2. Tensile data for the A212-B and A302-B steel for the three principal plate directions are presented (Figs. 8 and 9).

3. Complete reference stress-strain data for each steel in the unirradiated condition are presented (Figs. 11 and 12). The tensile strengths for the low nickel series and the nickel series of steels extend from about 60 ksi to 120 ksi; other tensile properties are typical for the respective classes of steel.

4. With exposure to neutron assumed to have a fission spectrum distribution, all steels were found to suffer properties modification. The changes in stress-strain curves are presented in detail (Figs. 14 through 20).

5. Selected fractures are described by fractographs (Figs. 29 and 30), which show that certain of the steels possess high reduction of area at the highest fluence levels studied while certain of the steels suffer brittle fracture under a like neutron exposure.

6. The analytic expressions for the true stress-natural strain curves for all irradiated conditions are presented (Eqs. (1) and (2)).

7. All numerical determinations and summaries of graphical data are presented in the Appendix.

Investigations of stress-strain responses of irradiated structural steels are continuing and will explore material performances at elevated temperatures and after neutron exposure at elevated (reactor service) temperatures. Experimental observations will be given in future summary reports.

ACKNOWLEDGMENTS

The NRL studies on the effects of irradiation on the tensile properties of reactor structural materials are supported by the Office of Naval Research, the Naval Ships System Command, the Army Nuclear Power Program, and the Atomic Energy Commission (Division of Reactor Development and Technology).

The authors wish to thank the members of the Reactor Materials Branch for their efforts toward the performance of materials irradiation experiments and the execution of material tests and evaluations.

REFERENCES

1. Stern, R.H., Jr., "The Coming Steels for Nuclear Pressure-Vessel Service," Nucleonics 25(No. 3):60-65 (Mar. 1967)

2. Steele, L.E., et al., "Irradiation Effects on Reactor Structural Materials, Quarterly Progress Report 1 February-30 April 1966," NRL Memorandum Report 1700, May 15, 1966

3. Trudeau, L.P., "Radiation Effects on Toughness of Ferritic Steels for Reactor Vessels," AEC-ASM Monograph Series on Metallurgy in Nuclear Technology, New York: Rowman and Littlefield, 1964

4. Nichols, R.W. and Harries, D.R., "Brittle Fracture and Irradiation Effects in Ferritic Pressure Vessel Steels," pp. 162-198 in ASTM STP 341, "Radiation Effects in Metals and Neutron Dosimetry," 1963

5. Harries, D.R. and Eyre, B.L., "Effects of Irradiation in Iron and Steels," pp. 105-119 in ASTM STP 380, "Flow and Fracture of Metals and Alloys in Nuclear Environment," 1965

6. Trozera, T.A. and Flynn, P.W., "Effects of Irradiation on A302-B Steel Subjected to a Multiaxial Stress Distribution," pp. 337-349 in ASTM STP 380, "Flow and Fracture of Metals and Alloys in Nuclear Environments," 1965

7. Cottrell, A.H., "Theory of Brittle Fracture in Steel and Similar Metals," Trans. Met. Soc. AIME 212:192-203 (1958)

8. Petch, N.J., "The Cleavage Strength of Polycrystals," JISI 174:25-28 (1953)

9. Steele, L.E. and Hawthorne, J.R., "Encapsulation Techniques for NRL Irradiation Effects Studies," NRL Memorandum Report 1481, Dec. 1963

10. Hawthorne, J.R. and Steele, L.E., "Systems and Techniques for In-Reactor Temperature Control of NRL Irradiation Experiments," NRL Memorandum Report 1486, Dec. 1963

11. Steele, L.E. and Hawthorne, J.R., "Neutron Embrittlement of Reactor Pressure Vessel Steels," NRL Report 5984, Oct. 22, 1963; and Chapter 16, pp. 366-409 in "Materials and Fuels for High-Temperature Nuclear Energy Applications," Cambridge, Mass:MIT Technology Press, 1964

12. Steele, L.E., "Practical Neutron Dosimetry for Steel Irradiation Studies," Special Report 69, The Iron and Steel Institute, London, England, 328-342, 1961

13. Serpan, C.Z., Jr. and Steele, L.E., "Neutron Spectral Considerations Affecting Projected Estimates of Radiation Embrittlement of the Army SM-1A Reactor Pressure Vessel," NRL Report 6474, Sept. 30, 1966

14. Serpan, C.Z., Jr. and Steele, L.E., "Damaging Neutron Exposure Criteria for Evaluating the Embrittlement of Reactor Pressure Vessel Steels in Different Neutron Spectra," NRL Report 6415, July 28, 1966; ASTM STP 426 (1967), pending publication

15. Serpan, C.Z., Jr., "Yankee Reactor Pressure Vessel Surveillance Notch Ductility Performance of the Vessel Steel and Maximum Service Fluence Determined from Exposures During Cores II, III, and IV," Trans. ASME (1967 Winter Meeting), pending publication

16. Serpan, C.Z., Jr. and Steele, L.E., "In-Depth Embrittlement of a Simulated Pressure Vessel Wall of A302-B Steel," NRL Report 6151, Sept. 4, 1964; also pp. 350-363 in ASTM STP 380, "Flow and Fracture of Metals and Alloys in Nuclear Environments," 1965

17. Steele, L.E. and Hawthorne, J.R., "New Information on Neutron Embrittlement and Embrittlement Relief of Reactor Pressure Vessel Steels," NRL Report 6160, Oct. 6, 1964; also pp. 283-311 in ASTM STP 380, "Flow and Fracture of Metals and Alloys in Nuclear Environments," 1965

18. Steele, L.E., Hawthorne, J.R., and Gray, R.A., Jr., "Neutron Irradiation Embrittlement of Several Higher Strength Steels," NRL Report 6419, Sept. 7, 1966; ASTM STP 426 (1967), pending publication

19. Hawthorne, J.R. and Steele, L.E., "Initial Evaluation of Metallurgical Variables as Possible Factors Controlling the Radiation Sensitivity of Structural Steels," NRL Report 6420, Sept. 29, 1966; ASTM STP 426 (1967), pending publication

20. Hawthorne, J.R., et al., "Irradiation Effects on Reactor Structural Materials, Quarterly Progress Report - 1 November 1966-31 January 1967," NRL Memorandum Report 1753, Feb. 15, 1967

21. Hawthorne, J.R., et al., "Irradiation Effects on Reactor Structural Materials, QPR - 1 February-30 April 1967," NRL Memorandum Report 1780, May 15, 1967

22. Ludwik, P., "Elemente der technologischen Mechanik," Berlin:Springer, 1909

23. Hill, R., "The Mathematical Theory of Plasticity," New York and Oxford:Clarendon Press, 1950

24. Hollomon, J.H., "Tensile Deformation," Trans. AIME 162:268-289 (1945)

25. Low, J.R., unpublished information, see Ref. 24, footnote, p. 280

APPENDIX

SUMMARY TABLES AND PLOTS OF DATA ENVELOPES

Following in this appendix are fourteen tables summarizing the tensile data for the seven steels evaluated, and 22 plots of data envelopes of stress versus natural strain for the steels under the various irradiation conditions. Each table summarizes the results for a specific lot of the steel designated, the compositions of the lots being given in Table 1 (except for the lot of Table A11).

Table A1
Tensile Data for A212-B Steel for Specimens Oriented in the Plate as Indicated

Specimen Number	0.2% Yield Strength (ksi)	Tensile Strength (ksi)	Specimen Orientation	Percent Elongation	Percent Reduction of Area	Natural Strain at Maximum Load	Calculated Fatigue Crack Notch Strength (ksi)	
							From Yield Strength	From Tensile Strength
1	52.0	82.6	L	—	64.2	0.18		
2	49.8	80.8	L	—	67.0	0.17		
3	45.3	74.0	L	—	55.0	—		
5	54.3	85.3	L	—	58.7	—		
7	—	84.8	L	30.6	58.7	—		
8	45.5	74.0	L	—	66.9	—		
9	50.6	81.0	L	31.7	62.7	—		
Av:	49.6	80.4		31.2	61.9	0.18	73.6	119.3
1	51.3	80.8	Tr	—	52.3	—		
3	47.6	77.0	Tr	—	53.4	—		
4		83.5	Tr	31.9	60.2	0.13		
6		82.3	Tr	—	48.4	—		
8	53.8	85.2	Tr	26.7	54.5	—		
9		73.6	Tr	31.9	49.0	—		
10		70.9	Tr	42.5	58.7	0.18		
Av:	50.9	79.0		33.3	53.8	0.16	75.5	117.3
1	43.8	70.3	Th	11.5	11.6	0.13		
2	44.0	67.5	Th	10.0	8.5	—		
4	44.3	73.0	Th	13.3	10.8	—		
5	45.5	52.0	Th	11.5	7.8	—		
Av:	44.4	70.7		11.6	9.7	0.13	65.9	104.9

Table A2
Tensile Data for A212-B Steel Irradiated as Indicated

Specimen Number	Irradiation Temperature (°F)	Neutron Exposure (10^{19} n/cm^2 (> 1 Mev))	0.2% Yield Strength (ksi)	Tensile Strength (ksi)	Hardness Rockwell B	Percent Elongation	Percent Reduction in Area	Natural Strain at Maximum Load	Calculated Fatigue Crack Notch Strength (ksi)	
									From Yield Strength	From Tensile Strength
18	—	—	43.8	72.8	—	39.4	54.5	0.19		
19			44.1	73.3	—	40.3	64.5	0.17		
20			44.0	72.8	—	36.8	63.7	0.20		
28			49.9	80.1	—	33.0	63.7	0.20		
29			47.3	78.8	—	33.6	62.2	0.19		
102			44.6	73.1	—	32.9	—	0.20		
106			—	—	—	32.6	—	—		
Av:			45.6	75.2	—	35.5	61.7	0.19	67.7	111.5
78	240 (C15-C)	0.75	83.7	88.2	95	19.8	54.1	0.10		
Av:			83.7	88.2	95	19.8	54.1	0.10	124.2	138.9
75	240 (C15-B)	1.55	92.6	102.2	104	21.3	56.3	0.10		
Av:			92.6	102.2	104	21.3	56.3	0.10	137.4	151.7
31	250 (S-20)	2.2	99.8	102.2	99	—	45.4	0.08		
45			00.2	102.8	98	—	36.9	0.06		
Av:			00.0	102.5	99	—	41.2	0.07	148.4	152.1
21	240 (C-32)	2.35	99.8	100.2	—	—	54.5			
22				97.6	—	—	54.5			
Av:			99.8	98.9	—	—	54.5		148.1	146.8
14	200 (S-29)	9.6	111.5	114.0	—	—	46.0	0.02		
13			112.8	113.8	—	—	42.0	0.02		
Av:			112.2	113.9	—	—	44.0	0.02	166.4	169.0
71	430 + 200	2.5	95.1	108.5	101	18.7	51.8	0.14		
69	(C-11)		100.0	100.8	99	12.7	38.6			
65			93.5	106.9	99	19.4	51.8	0.12		
Av:			96.2	105.4	100	16.9	47.4	0.13	142.8	156.4
72	510 + 275	2.1	87.6	104.5	98	21.8	54.8	0.15		
70	(C-12)		100.0	100.4	98	13.9	54.1			
66			97.0	99.0	97	18.0	54.8	0.06		
8			88.2	105.3	101	20.7	54.8	0.15		
Av:			93.2	102.3	99	18.6	54.6	0.12	138.3	151.8
4	650	4.0		89.0	—	—				
7	(C(55)27)			91.6	—	—	50.0	0.15		
9			65.2	87.8	—	—	56.5	0.15		
10				87.0	—	—	52.0	0.20		
Av:			65.2	88.9	—	—	52.8	0.17	96.8	131.9

Table A3
Tensile Data for A212-B Steel Irradiated as Indicated

Specimen Number	Irradiation Temperature (°F)	Neutron Exposure (10^{19} n/cm^2 (> 1 Mev))	0.2% Yield Strength (ksi)	Tensile Strength (ksi)	Percent Elongation	Percent Reduction in Area	Natural Strain at Maximum Load	Calculated Fatigue Crack Notch Strength (ksi)	
								From Yield Strength	From Tensile Strength
2	—	—	47.1	78.0	36.5	59.8	0.20		
3			54.0	87.0	38.3	61.0	0.20		
5			43.3	73.5	41.1	63.8	0.20		
6			51.3	83.8	37.7	61.0	0.20		
8				73.5		65.2	0.18		
9			44.0	74.9	40.4	64.6	0.20		
10			51.0	83.8	45.0	62.0	0.20		
12			43.0	73.6		67.0	0.18		
14			50.0	81.1	38.8	66.6	0.17		
15			58.6	92.8	33.8	60.0	0.18		
Av:			49.1	80.2	39.0	63.1	0.19	72.9	119.0
17	240	0.85	82.0	83.8	--	59.0	--		
19	(C-48)		85.5	87.5	--	60.0	0.10		
Av:			83.8	85.7	--	60.0	0.10	124.3	127.1

Table A4
Tensile Data for A212-B Steel for Specimens Oriented in the Plate as Indicated

Specimen Number	0.2% Yield Strength (ksi)	Tensile Strength (ksi)	Specimen Orientation	Percent Elongation	Percent Reduction of Area	Natural Strain at Maximum Load	Calculated Fatigue Crack Notch Strength (ksi)	
							From Yield Strength	From Tensile Strength
3	41.8	79.8	L	35.3	64.0	0.24		
4	42.0	79.1	L	34.8	56.0	0.22		
11	41.3	75.5	L	36.1	63.0	0.26		
12	44.3	79.5	L	35.7	54.5	0.26		
23	41.5	75.8	L	35.0	59.0	0.24		
24	43.9	77.1	L	35.8	60.0	0.24		
29	42.3	75.5	L	35.4	58.0	0.26		
30	43.8	76.1	L	35.5	61.0	0.22		
Av:	42.6	77.3		35.5	59.4	0.24	63.2	114.7

Table A5
Tensile Data for A302-B Steel for Specimens Oriented in the Plate as Indicated

Specimen Number	0.2% Yield Strength (ksi)	Tensile Strength (ksi)	Specimen Orientation	Percent Elongation	Percent Reduction of Area	Natural Strain at Maximum Load	Calculated Fatigue Crack Notch Strength (ksi)	
							From Yield Strength	From Tensile Strength
1	67.9	91.2	L	27.9	64.5	0.12		
2	65.1	86.6	L	28.8	64.0	0.13		
3	64.0	84.5	L	31.1	64.0	0.13		
4	65.8	87.3	L	28.3	63.0	0.12		
5	68.5	92.0	L	27.5	59.8	0.11		
8	63.8	84.5	L	32.6	64.5	0.13		
9	67.0	89.8	L	26.5	62.5	0.12		
10	69.3	91.8	L	26.5	64.0	0.12		
Av:	66.4	88.5		28.7	63.3	0.12	98.6	131.3
1	67.3	90.3	Tr	23.8	46.1	0.11		
4	64.5	87.0	Tr	26.7	51.7	0.13		
Av:	65.9	88.7		25.3	48.9	0.12	97.8	131.6
1	63.3	83.4	Th	13.5	13.0	0.10		
3	64.0	84.0	Th	14.3	17.4	0.12		
4	65.8	84.3	Th	8.6	9.3	0.07		
6	64.0	82.8	Th	—	10.0	0.07		
7	64.0	82.1	Th	—	5.5	—		
Av:	64.2	83.3		12.1	11.5	0.09	95.3	123.7

Table A6
Tensile Data for A302-B Steel Irradiated as Indicated

Specimen Number	Irradiation Temperature (°F)	Neutron Exposure (10^{19} n/cm^2 (> 1 Mev))	0.2% Yield Strength (ksi)	Tensile Strength (ksi)	Hardness Rockwell B	Percent Elongation	Percent Reduction in Area	Natural Strain at Maximum Load	Calculated Fatigue Crack Notch Strength (ksi)	
									From Yield Strength	From Tensile Strength
1			68.3	90.6	—	30.5	65.2	0.08		
4			68.0	90.8	—	28.2	67.3	0.09		
17			68.5	91.7	—	—	63.7	0.11		
18			79.0	104.0	—	—	61.7	0.10		
20			71.5	94.5	—	24.0	61.2	0.12		
23			67.8	90.4	—	27.7	65.6	0.11		
24			77.5	102.1	—	27.5	61.2	0.13		
25			68.0	91.0	—	30.2	65.5	0.12		
27			77.0	100.8	—	28.8	63.1	0.13		
28			68.0	90.0	—	26.9	66.0	0.12		
Av:			71.4	94.6	—	28.0	64.0	0.12	105.9	140.4
90	240 (C25-B)	2.0	114.8	116.7	103	11.3	52.6	—		
Av:			114.8	116.7	103	11.3	52.6	—	170.4	173.2
10	240 (C-32)	2.3	122.5	122.6	—	—	50.0	< 0.02		
22			118.0	118.2	—	—	50.0	< 0.02		
Av:			120.3	120.4	—	—	50.0	< 0.02	178.5	178.7
11	250 (S-20)	2.2	114.6	116.7	104	—	47.0	< 0.03		
20			112.4	114.0	102	—	44.0	0.01		
Av:			113.5	115.4	103	—	46.0	0.02	168.4	171.1
60	250 (S-26)	7.0	—	118.5	102	—	—	—		
52			118.7	118.7	102	3.0	—	< 0.02		
Av:			118.7	118.6	102	3.0	—	< 0.02	176.2	176.0
15	200 (S-29)	9.6	133.6	133.8	—	—	44.0	< 0.02		
12			134.8	135.0	—	—	45.5	< 0.02		
Av:			134.2	134.4	—	—	45.0	< 0.02	199.2	199.5
53	600 (C-20)	2.3	98.3	112.8	102	—	45.0	0.13		
79		5.7	100.6	117.1	103	—	49.0	0.11		
Av:			99.5	115.0	103	—	47.0	0.12	147.7	170.6

Table A7
Tensile Data for A302-B Steel Irradiated as Indicated

Specimen Number	Irradiation Temperature (°F)	Neutron Exposure (10^{19} n/cm^2 (> 1 Mev))	0.2% Yield Strength (ksi)	Tensile Strength (ksi)	Percent Elongation	Percent Reduction in Area	Natural Strain at Maximum Load	Calculated Fatigue Crack Notch Strength (ksi)	
								From Yield Strength	From Tensile Strength
1	—	—	66.0	88.6	—	66.5	0.09		
2			69.5	91.3	29.7	61.0	0.13		
4			78.4	91.0	31.4	66.9	0.13		
6			69.6	93.2	24.2	64.6	0.11		
7			71.0	94.3	28.9	59.0	0.14		
9			70.0	92.0	22.3	54.5	0.12		
10			—	93.3	27.9	62.1	0.13		
13			70.0	92.9	25.7	64.5	0.09		
15			71.8	93.8	27.2	60.0	0.13		
16			70.2	93.2	26.9	63.1	0.11		
Av:			70.7	92.4	27.1	62.2	0.12	105.0	137.1
20	240	0.85	100.2	102.4	—	59.0	0.10		
26	(C-48)		102.0	102.4	—	54.5	0.07		
Av:			101.1	102.4	—	57.0	0.09	150.0	152.0
21	240	1.4	111.8	111.8	15.5	49.0	< 0.02		
23	(C28-66C)		112.5	112.5	15.3	49.0	< 0.02		
Av:			112.2	112.2	15.4	49.0	< 0.02	166.4	166.4

Table A8
Tensile Data for A302-B Steel for Specimens Oriented in the Plate as Indicated

Specimen Number	0.2% Yield Strength (ksi)	Tensile Strength (ksi)	Specimen Orientation	Percent Elongation	Percent Reduction of Area	Natural Strain at Maximum Load	Calculated Fatigue Crack Notch Strength (ksi)	
							From Yield Strength	From Tensile Strength
2	83.5	103.5	L	28.1	61.2	0.12		
12	72.8	94.0	L	25.8	61.2	0.11		
19	75.5	96.0	L	26.6	62.7	0.10		
39	79.5	100.3	L	26.3	63.6	0.12		
Av:	77.8	98.5		26.7	62.2	0.11	115.5	146.1

Table A9
Tensile Data for T-1 Steel Irradiated as Indicated

Specimen Number	Irradiation Temperature (°F)	Neutron Exposure (10^{19} n/cm^2 (> 1 Mev))	0.2% Yield Strength (ksi)	Tensile Strength (ksi)	Percent Elongation	Percent Reduction in Area	Natural Strain at Maximum Load	Calculated Fatigue Crack Notch Strength (ksi)	
								From Yield Strength	From Tensile Strength
26	—	—	—	114.3	—	60.7	0.05		
29			110.0	120.7	18.8	52.6	0.08		
30			107.0	118.6	20.0	67.0	0.06		
38			106.9	118.5	17.3	59.1	0.09		
Av:			108.0	118.0	18.7	59.9	0.07	160.3	175.2
6	240	2.3	147.8	148.5	—	49.0	<0.02		
7	(C-32)		150.0	150.5	—	47.5	<0.02		
Av:			148.9	149.5	—	48.3	<0.02	221.0	221.9
18	200	9.6	165.5	166.2	—	42.0	<0.02		
10	(S-29)		161.2	162.0	—	46.0	<0.02		
Av:			163.4	164.1	—	44.0	<0.02	242.4	243.5

Table A10
Tensile Data for A350-LF1 Steel Irradiated as Indicated

Specimen Number	Irradiation Temperature (°F)	Neutron Exposure (10^{19} n/cm^2 (> 1 Mev))	0.2% Yield Strength (ksi)	Tensile Strength (ksi)	Hardness Rockwell B	Percent Elongation	Percent Reduction in Area	Natural Strain at Maximum Load	Calculated Fatigue Crack Notch Strength (ksi)	
									From Yield Strength	From Tensile Strength
23			48.0	64.8	—	35.5	78.8	0.22		
17			46.2	64.3	—	36.4	79.6	0.27		
Av:			47.1	64.6	—	36.0	79.2	0.25	70.0	95.9
5	240	0.70	84.1	85.7	95	12.0	57.8	0.10		
82	(C-17)		77.6	81.9	93	21.9	57.8	0.11		
7			86.1	87.6	96	13.9	43.8	—		
Av:			82.6	85.1	95	15.9	53.1	0.11	122.6	126.3
9	240	2.35	104.4	104.8	—	—	55.5	0.02		
11	(C-32)	2.35	105.0	106.0	—	—	57.7	0.02		
Av:			104.7	105.4	—	—	56.6	0.02	155.4	156.4
1	200	9.6	123.2	124.5	—	—	8.0	0.02		
3	(S-29)		117.5	119.8	—	—	15.5	0.02		
Av:			120.4	122.2	—	—	11.8	0.02	178.6	181.3
3	430	3.1	99.45	107.9	100	18.5	57.0	0.14		
11	(C-22)	3.1	101.8	108.8	103	19.1	56.3	0.14		
16		3.1	104.9	107.9	101	17.0	54.8	0.06		
Av:			102.1	108.2	101	18.2	56.0	0.11	151.5	165.6
4	430 + 200	2.5	98.4	108.7	100	20.0	59.1	0.17		
8	(C-11)		104.7	105.3	101	—	41.2	0.03		
10			101.0	108.4	101	18.3	55.6	0.14		
15			111.0	111.4	101	11.4	57.8	—		
Av:			103.8	108.5	101	16.6	53.4	0.12	154.0	161.0

Table A11
Tensile Data for A350-LF1 Steel for Specimens Oriented in the Plate as Indicated

Specimen Number	0.2% Yield Strength (ksi)	Tensile Strength (ksi)	Specimen Orientation	Percent Elongation	Percent Reduction of Area	Natural Strain at Maximum Load	Calculated Fatigue Crack Notch Strength (ksi)	
							From Yield Strength	From Tensile Strength
1	54.25	77.2	L	34.6	75.0	0.16		
4	49.9	74.0	L	37.7	71.4	0.15		
7	50.6	73.0	L	34.7	71.7	0.22		
10	50.25	73.3	L	36.4	74.6	0.20		
11	53.5	75.8	L	37.2	70.0	0.15		
12	51.25	73.0	L	36.0	72.6	0.19		
15	49.3	71.5	L	35.5	73.3	0.19		
18	50.6	72.6	L	37.6	71.3	0.22		
20	49.25	71.5	L	37.4	70.0	0.19		
21	54.8	76.1	L	34.7	70.0	0.15		
23	51.8	72.5	L	34.6	69.1	0.22		
25	51.0	71.9	L	36.5	61.1	0.19		
28	51.9	73.2	L	39.9	67.9	0.22		
30	50.25	71.4	L	37.0	68.3	0.19		
Av:	51.3	73.4		36.4	70.5	0.19	76.2	108.9

Table A12
Tensile Data for A350-LF3 Steel Irradiated as Indicated

Specimen Number	Irradiation Temperature (°F)	Neutron Exposure (10^{19} n/cm^2 (> 1 Mev))	0.2% Yield Strength (ksi)	Tensile Strength (ksi)	Hardness Rockwell B	Percent Elongation	Percent Reduction in Area	Natural Strain At Maximum Load	Calculated Fatigue Crack Notch Strength (ksi)	
									From Yield Strength	From Tensile Strength
13	—	—	57.5	81.5	—	33.0	69.5	0.13		
15			60.2	84.0	—	35.2	63.1	0.19		
19			56.0	80.8	—	32.3	71.0	0.10		
36			58.0	81.2	—	32.3	71.7	—		
37			61.3	84.0	—	32.8	64.6	0.19		
38			58.5	81.5	—	32.1	71.8	0.09		
Av:			58.6	82.2	—	33.0	68.6	0.14	86.9	122.0
19	240 (C17)	0.70	98.3	100.6	100	16.5	59.0	0.03		
5			99.2	102.8	—	16.5	52.0	0.08		
Av:			98.8	101.7	100	16.5	55.5	0.06	146.6	150.9
40	240 (C15-C)	0.75	97.3	100.6	100	17.7	52.0	0.03		
Av:			97.3	100.6	100	17.7	52.0	0.03	144.4	149.3
20	240 (C-48)	0.85	105.0	106.0	—	—	61.0	~0.02		
22			102.3	102.4	—	—	57.4	0.03		
Av:			103.7	104.2	—	—	59.2	<0.03	153.9	154.6
4	240 (C15-B)	1.55	103.0	104.2	101	10.8	52.0	—		
Av:			103.0	104.2	101	10.8	52.0		152.9	154.6
11	240 (C-32)	2.3	123.8	124.0	—	—	54.5	<0.03		
9			126.5	126.5	—	—	55.5	<0.02		
Av:			125.2	125.3	—	—	55.0	<0.03	185.8	185.9
39	240	6.99	126.8	126.8	—	—	45.5	—		
41			130.2	130.2	—	—	42.0	—		
Av:			128.5	128.5	—	—	44.0	—		
1	200 (S-29)	9.6	133.9	133.9	—	—	2.4	—		
6			139.8	144.0	—	—	15.5	<0.05		
2			—	—	—	—	16.8	<0.02		
Av:			136.9	139.0	—	—	11.6	<0.03	203.2	206.3
3	510 (C-12)	2.5	114.0	123.8	104	21.0	55.0	0.11		
12			106.7	120.5	104	18.9	52.0	0.14		
15			122.6	123.2	101	7.8	56.3	—		
21			124.2	125.0	105	11.8	49.0	—		
Av:			116.9	123.1	104	14.9	53.0	0.13	173.5	182.7
101	600 (C-20)	5.7	101.4	106.3	104	14.7	52.0	0.17		
107			103.4	119.1	102	—	36.0	0.13		
Av:			102.4	112.7	103	14.7	44.0	0.15	152.0	167.3

Table A13
Tensile Data for HY-80 Steel Irradiated as Indicated

Specimen Number	Irradiation Temperature (°F)	Neutron Exposure (10^{19} n/cm^2 (> 1 Mev))	0.2% Yield Strength (ksi)	Tensile Strength (ksi)	Hardness Rockwell B	Percent Elongation	Percent Reduction in Area	Natural Strain at Maximum Load	Calculated Fatigue Crack Notch Strength (ksi)	
									From Yield Strength	From Tensile Strength
7			89.8	106.0	--	27.2	75.7	0.07		
22			82.1	96.3	--	25.6	78.3	0.10		
27			87.8	103.5	--	28.4	77.3	0.11		
28			91.5	106.6	--	--	57.6	0.11		
30			88.8	104.5	--	29.5	63.1	0.11		
31			85.0	101.8	--	29.2	78.2	0.09		
33			93.5	108.5	--	31.1	67.3	0.10		
34			--	105.0	--	--	73.3	0.08		
36			88.0	103.9	--	30.1	76.2	0.11		
40			88.0	103.4	--	21.1	59.0	--		
Av:			88.3	104.0	--	27.8	70.6	0.10	131.0	154.3
18	240 (C48)	0.85	111.6	112.2	--	--	68.0	<0.02		
21			113.0	113.5	--	--	68.0	<0.02		
Av:			112.3	112.9	--	--	68.0	<0.02	166.7	167.6
30	240 (C25-B)	2.0	134.4	136.4	111	10.4	--	--		
Av:			134.4	136.4	111	10.4	--	--	192.1	194.8
1	240 (C32)	2.3	140.5	141.5	--	--	62.8	<0.02		
16			142.0	142.5	--	--	62.8	<0.02		
Av:			141.3	142.0	--	--	62.8	<0.02	209.6	210.7
22	250 (S-26)	7.0	157.2	158.0	111	--	11.8	--		
25			150.3	150.9	109	--	15.0	--		
Av:			153.8	154.5	110	--	13.4	--	228.3	229.2
8	250 (S-29)	9.0	159.6	160.4	--	--	13.8	<0.02		
14			167.0	168.2	--	--	10.8	<0.02		
Av:			163.3	164.3	--	--	12.3	<0.02	242.4	243.8
3	650 (C55-27)	4.0	95.0	110.6	--	--	--	--		
Av:			95.0	110.6	--	--	55.6	--	141.0	164.1

Table A14
Tensile Data for A353 Steel Irradiated as Indicated

Specimen Number	Irradiation Temperature (°F)	Neutron Exposure (10^{19} n/cm^2 (> 1 Mev))	0.2% Yield Strength (ksi)	Tensile Strength (ksi)	Hardness Rockwell B	Percent Elongation	Percent Reduction in Area	Natural Strain at Maximum Load	Calculated Fatigue Crack Notch Strength (ksi)	
									From Yield Strength	From Tensile Strength
13	—	—	94.2	111.0	—	28.6	68.3	0.09		
14	—	—	99.75	114.0	—	27.6	62.7	0.14		
16	—	—	92.6	109.5	—	28.7	69.2	—		
23	—	—	98.75	114.25	—	31.7	66.0	0.13		
31	—	—	98.25	113.75	—	29.7	58.2	0.13		
32	—	—	93.5	110.0	—	28.6	69.2	0.13		
Av:			96.2	112.1	—	29.2	65.6	0.12	142.8	166.4
8	240	2.35	141.6	145.5	103	17.8	54.5	< 0.02		
10	240	2.35	141.0	143.5	—	—	56.5	—		
Av:			141.3	144.5	103	17.8	55.5	< 0.02	209.7	214.4
2	200	9.5	164.0	165.5	—	—	19.6	< 0.02		
4	200	9.5	170.0	172.2	—	—	13.8	< 0.02		
Av:			167.0	168.9	—	—	16.7	< 0.02	247.8	250.6

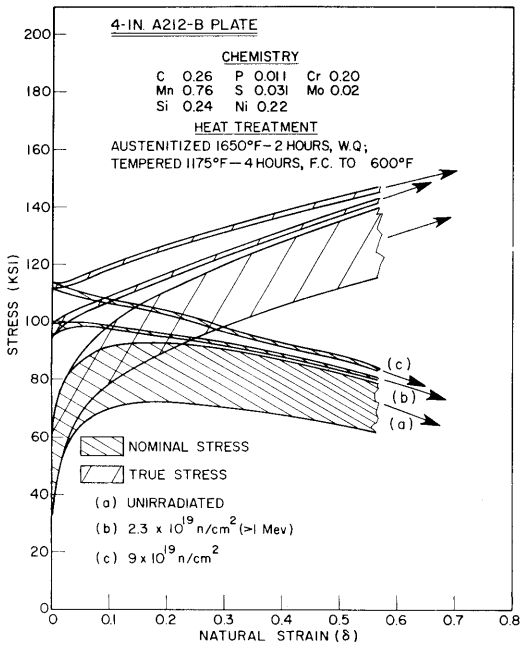

Fig. A1 - True stress-natural strain and nominal stress-natural strain maximum and minimum data envelopes for A212-B steel plate for indicated radiation exposures at < 250°F

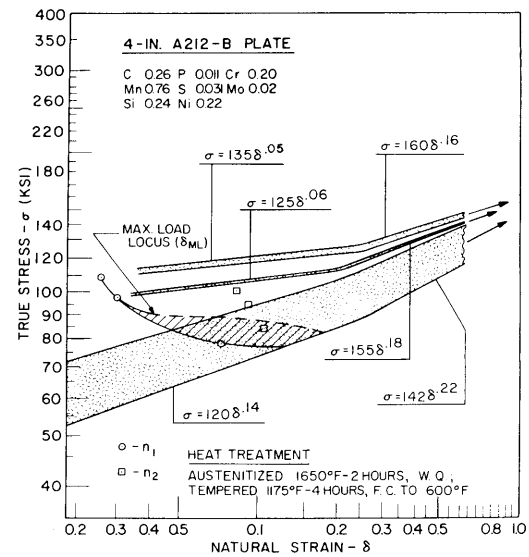

Fig. A2 - True stress-natural strain data envelopes for A212-B steel plate in ln-ln coordinates. The analytic expression for each curve segment is given for true stress in ksi.

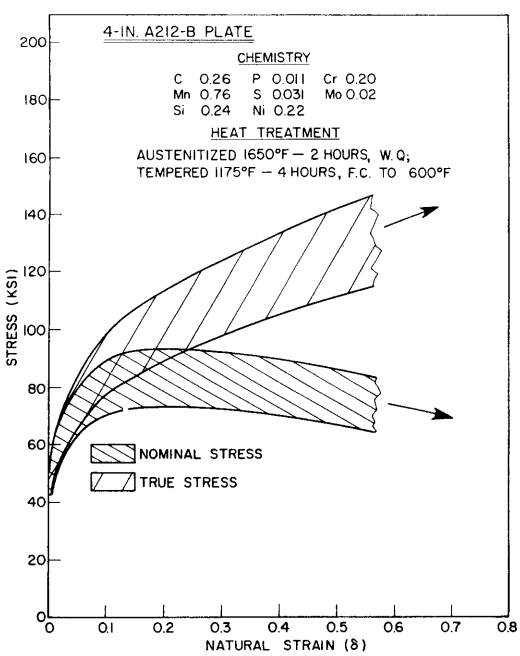

Fig. A3 - True stress-natural strain and nominal stress-natural strain maximum and minimum data envelopes for one set of unirradiated specimens of A212-B steel plate

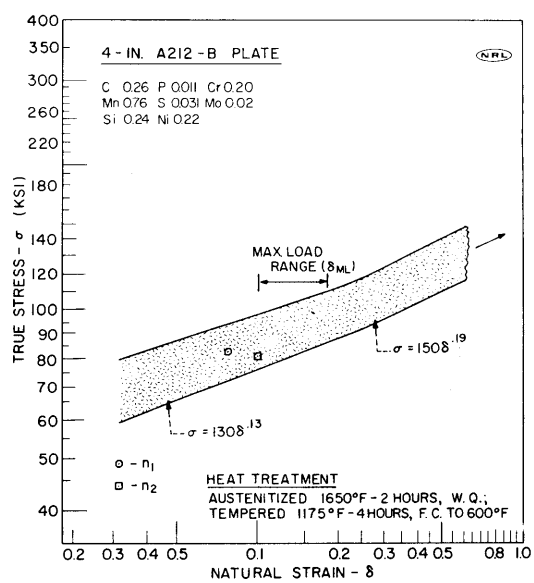

Fig. A4 - True stress-natural strain data envelope for one set of unirradiated specimens of A212-B steel plate in ln-ln coordinates

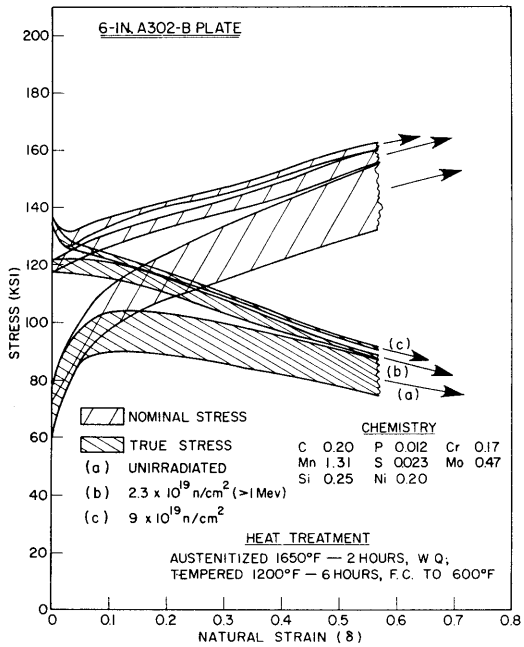

Fig. A5 - True stress-natural strain and nominal stress-natural strain maximum and minimum data envelopes for A302-B steel plate for indicated radiation exposures at < 250°F

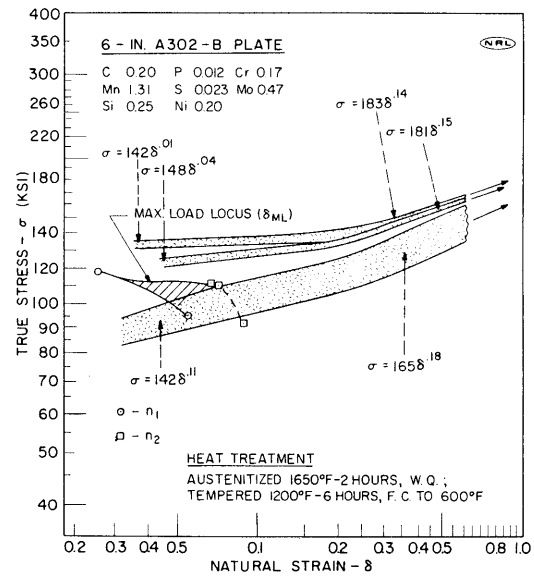

Fig. A6 - True stress-natural strain data envelopes for A302-B steel plate in ln-ln coordinates. The analytic expression for each curve segment is given for true stress in ksi.

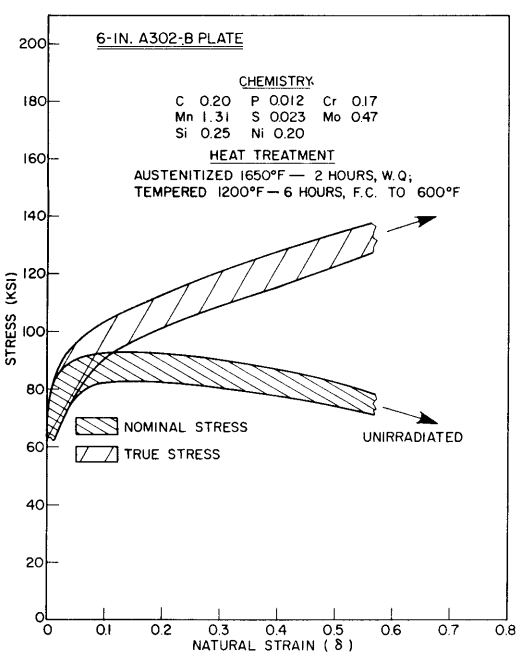

Fig. A7 - True stress-natural strain and nominal stress-natural strain maximum and minimum data envelopes for a second lot of unirradiated specimens of A302-B steel plate

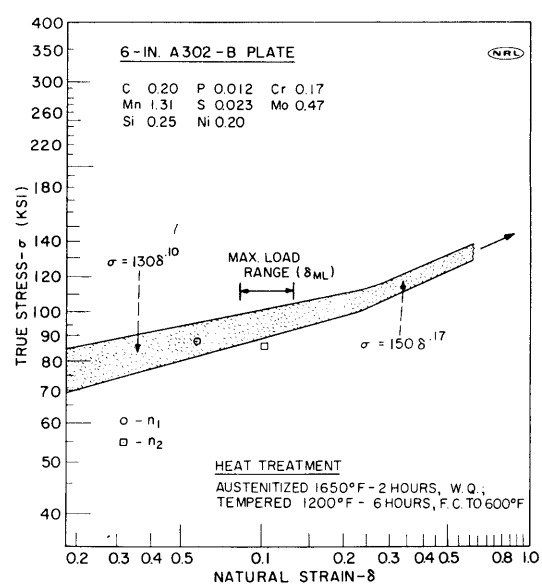

Fig. A8 - True stress-natural strain data envelope for a second lot of unirradiated specimens of A302-B steel plate in ln-ln coordinates

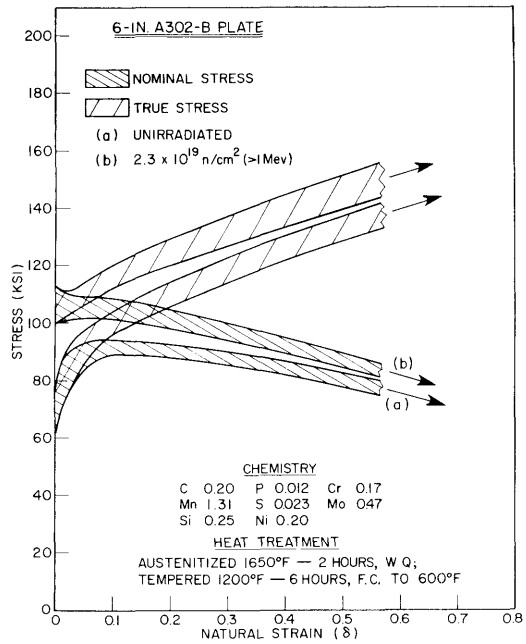

Fig. A9 - True stress-natural strain and nominal stress-natural strain maximum and minimum data envelopes for a third lot of specimens of A302-B steel plate. The indicated radiation exposure was at < 250°F.

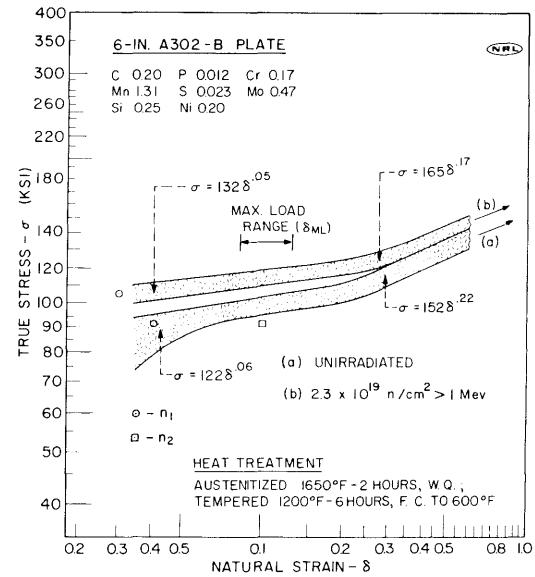

Fig. A10 - True stress-natural strain data envelopes for a third lot of specimens of A302-B steel plate in ln-ln coordinates. The indicated radiation exposure was at < 250°F. The analytic expression for each curve segment is given for true stress in ksi.

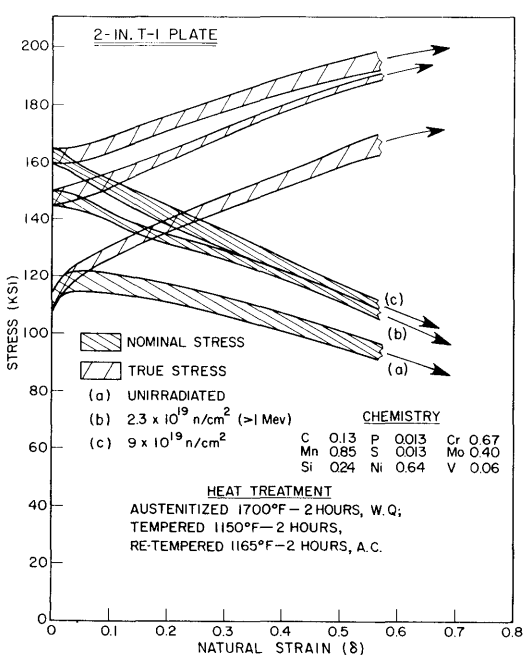

Fig. A11 - True stress-natural strain and nominal stress-natural strain maximum and minimum data envelopes for T-1 steel plate for indicated radiation exposures at < 250°F

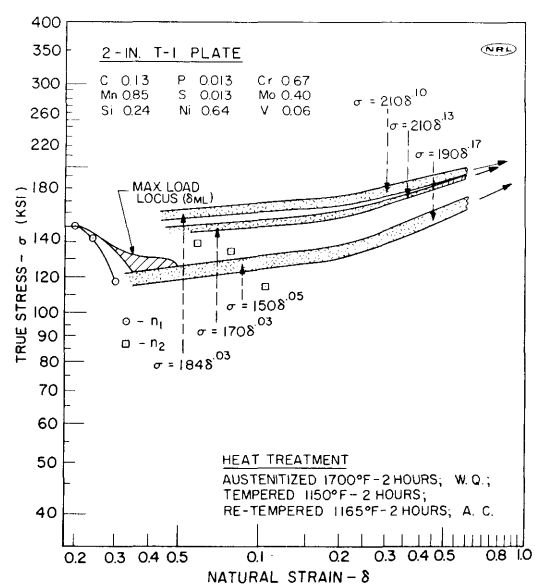

Fig. A12 - True stress-natural strain data envelopes for T-1 steel plate in ln-ln coordinates. The analytic expression for each curve segment is given for true stress in ksi.

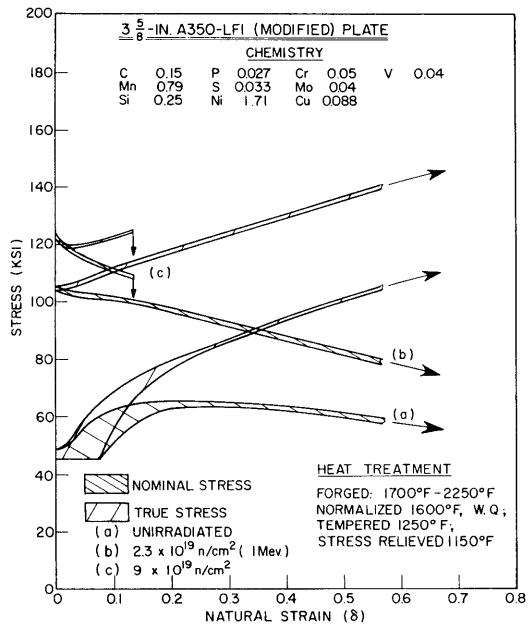

Fig. A13 - True stress-natural strain and nominal stress-natural strain maximum and minimum data envelopes for A350-LF1 (Modified) plate for indicated radiation exposures at > 250°F

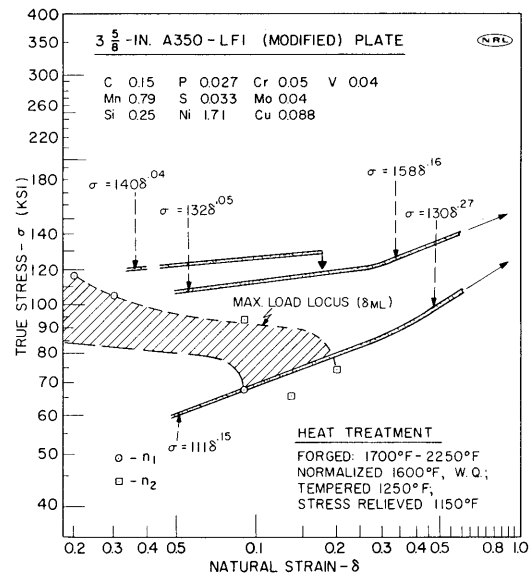

Fig. A14 - True stress-natural strain data envelopes for A350-LF1 (modified) steel plate in ln-ln coordinates. The analytic expression for each curve segment is given for true stress in ksi.

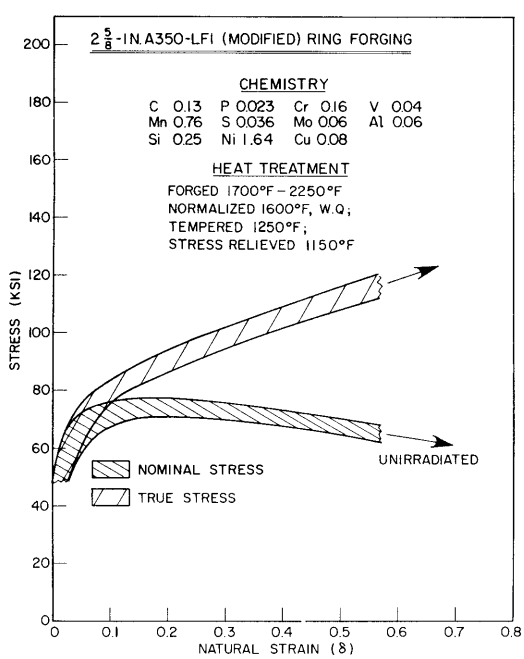

Fig. A15 - True stress-natural strain and nominal stress-natural strain maximum and minimum data envelopes for unirradiated A350-LF1 (Modified) steel ring forging

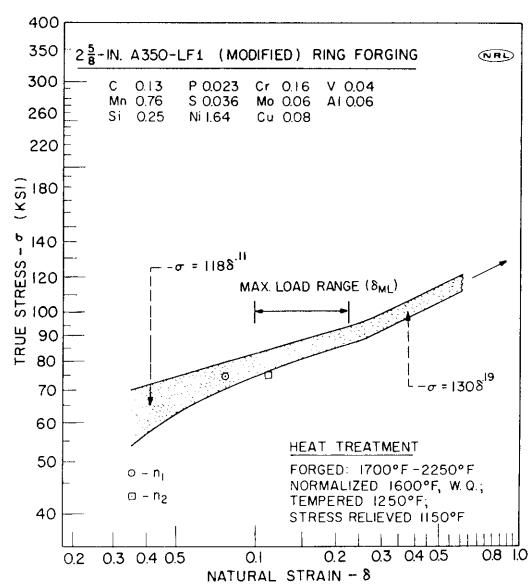

Fig. A16 - True stress-natural strain data envelopes for A350-LF1 (Modified) steel ring forging in ln-ln coordinates. The analytic expression for each curve segment is given for true stress in ksi.

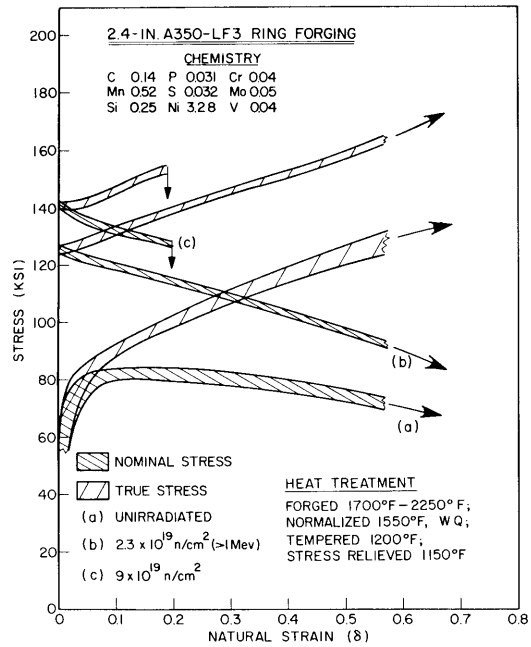

Fig. A17 - True stress-natural strain and nominal stress-natural strain maximum and minimum data envelopes for A350-LF3 steel ring forging for indicated radiation exposures at <250°F

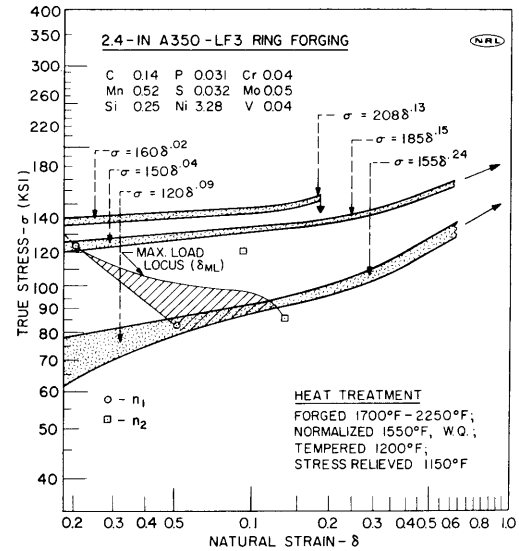

Fig. A18 - True stress-natural strain data envelopes for A350-LF3 steel ring forging in ln-ln coordinates. The analytic expression for each curve segment is given for true stress in ksi.

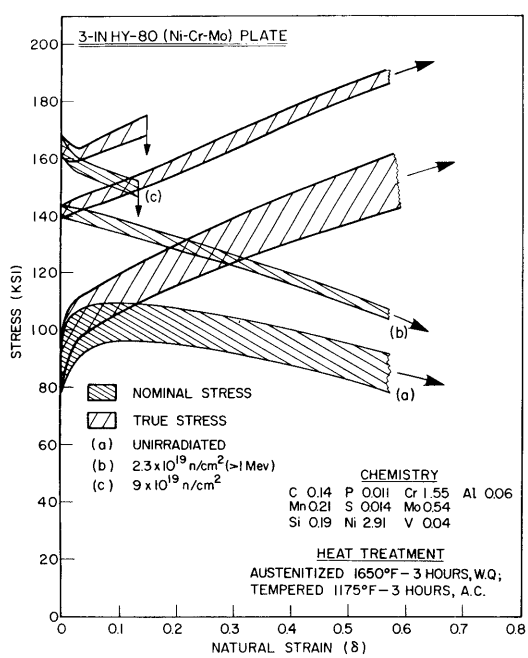

Fig. A19 - True stress-natural strain and nominal stress-natural strain maximum and minimum data envelopes for HY-80 steel plate for indicated radiation exposures at <250°F

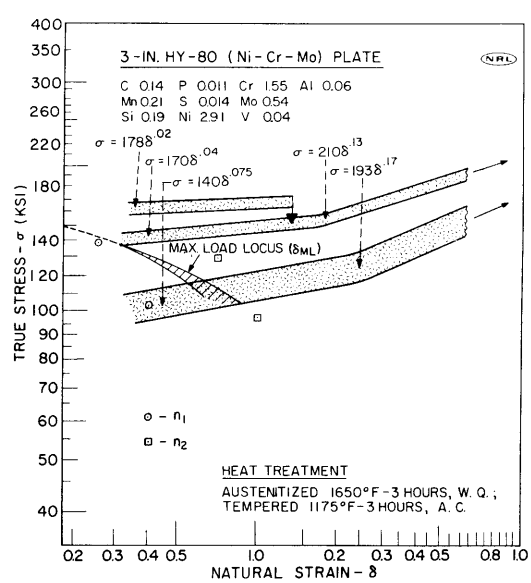

Fig. A20 - True stress-natural strain data envelopes for HY-80 steel plate in ln-ln coordinates. The analytic expression for each curve segment is given for true stress in ksi.

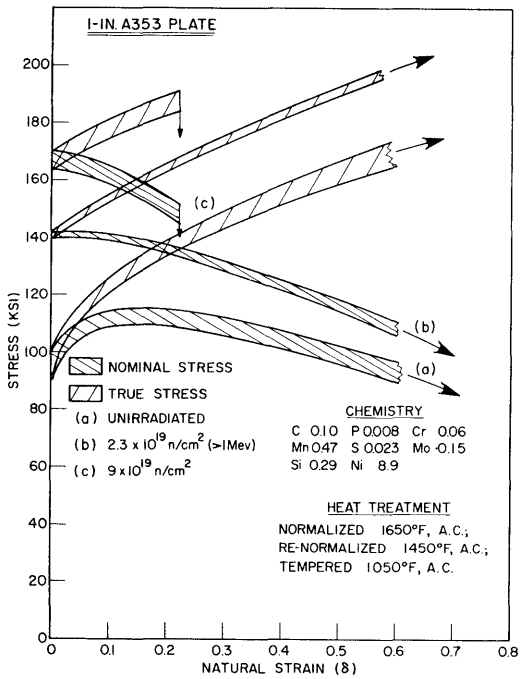

Fig. A21 - True stress-natural strain and nominal stress-natural strain maximum and minimum data envelopes for A353 steel plate for indicated radiation exposures at > 250°F

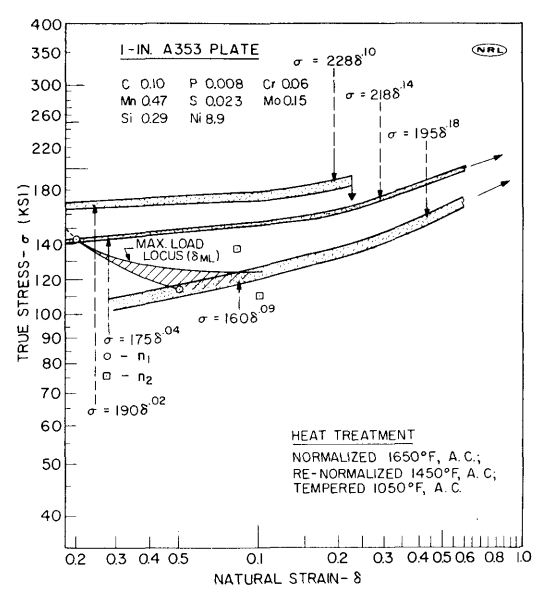

Fig. A22 - True stress-natural strain data envelopes for A353 steel plate in ln-ln coordinates. The analytic expression for each curve segment is given for true stress in ksi.

Security Classification

DOCUMENT CONTROL DATA - R & D

(Security classification of title, body of abstract and indexing annotation must be entered when the overall report is classified)

1. ORIGINATING ACTIVITY (Corporate author) Naval Research Laboratory Washington, D.C. 20390	2a. REPORT SECURITY CLASSIFICATION Unclassified 2b. GROUP

3. REPORT TITLE

THE TENSILE PROPERTIES OF SELECTED STEELS FOR USE IN NUCLEAR REACTOR PRESSURE VESSELS

4. DESCRIPTIVE NOTES (Type of report and inclusive dates)

A final report on one phase of the problem.

5. AUTHOR(S) (First name, middle initial, last name)

Klier, Eugene P., Hawthorne, J. R., and Steele, Lendell E.

6. REPORT DATE December 26, 1967	7a. TOTAL NO. OF PAGES 54	7b. NO. OF REFS 25
8a. CONTRACT OR GRANT NO NRL Problem M01-14 b. PROJECT NO RR007-01-46-5409 c. SF 020-01-05-0858 AT(49-5)-2110 d. USA-MIPR-ERG-3-67	9a. ORIGINATOR'S REPORT NUMBER(S) NRL Report 6649 9b. OTHER REPORT NO(S) (Any other numbers that may be assigned this report)	

10. DISTRIBUTION STATEMENT

This document has been approved for public release and sale; its distribution is unlimited.

11. SUPPLEMENTARY NOTES	12. SPONSORING MILITARY ACTIVITY Dept. of the Navy (Office of Naval Research and Naval Ship Systems Command) and Dept. of the Army (Army Nuclear Power Program)

13. ABSTRACT

Seven steels now used or having potential for use in the construction of nuclear reactor containment vessels were evaluated in uniaxial tension at 75°F following irradiation at < 250°F. Experiment irradiations involved neutron fluences up to 9.5×10^{19} n/cm^2 (> 1 Mev). Tensile properties of the A212-B, A302-B, A350-LF1 (Modified), A350-LF3, A353, T-1, and HY-80 (Ni-Cr-Mo) steels were determined as conventional tensile and yield strength and percent reduction of area. In addition, observed stress-strain relationships were plotted using both nominal stress-percent reduction of area coordinates and true stress-natural strain coordinates. Curves given in the latter coordinate system were also expressed in suitable analytic form. All individual tensile data were compiled in tabular form, and stress-strain curves were summarized as bands giving maximum and minimum properties behavior.

Limited metallographic and fractographic data were obtained to establish the metallurgical structures of the steels and to depict the transition from a ductile shear fracture to a brittle flat fracture at high neutron fluences for the more brittle steels.

DD FORM 1 NOV 65 1473 (PAGE 1)

S/N 0101-807-6801

Security Classification

Security Classification

14. KEY WORDS	LINK A ROLE	LINK A WT	LINK B ROLE	LINK B WT	LINK C ROLE	LINK C WT
Nuclear reactor						
Tensile properties						
Pressure vessel steels						
Radiation damage						
Neutron exposure						
Transition temperature						
Microstructure						
Fractures						
True stress-true strain						

DD FORM 1 NOV 65 1473 (BACK)
(PAGE 2)

Security Classification